

MOL #50765

**Facilitatory interplay in  $\alpha_{1A}$  and  $\beta_2$  adrenoceptor function reveals a non- $G_q$  signaling mode:  
implications for diversification of intracellular signal transduction**

Alicja J. Copik, Cynthia Ma, Alan Kosaka, Sunil Sahdeo, Andy Trane, Hoangdung Ho, Paul S.

Dietrich, Helen Yu, Anthony P. D. W. Ford, Donald Button and Marcos E. Milla\*

From the Inflammation Discovery (AJC, CM, SS, AT, APDWF, DB, MEM) and Discovery

Technologies (AK, HH, PSD, HY), Roche Palo Alto, Palo Alto, CA 94304

MOL #50765

Running title: functional coupling between  $\alpha$  and  $\beta$  adrenoceptors

\*Corresponding author:

Marcos E. Milla

3431 Hillview Avenue, Mailstop R2-101, Palo Alto, CA 94304

e-mail: [marcos.milla@roche.com](mailto:marcos.milla@roche.com)

Number of

- text pages: 51
- tables: 2
- figures: 8
- references: 56
- words in the Abstract: 302
- Introduction: 700
- Discussion: 2,209

### ABBREVIATIONS

$\alpha_{1A}$ -AR,  $\alpha_{1A}$ -adrenoceptor;  $\beta_2$ -AR,  $\beta_2$ -adrenoceptor;  $A_{2B}$ , Adenosine 2B receptor; ICYP, iodocyanopindolol; TCM, tetracysteine motif (CCPGCC); NECA, 5'-N-ethylcarboxamidoadenosine; CRAC channel,  $Ca^{2+}$  release-activated  $Ca^{2+}$  channel; SOC channel, store-operated  $Ca^{2+}$  channel; GPCR, G protein-coupled receptor; 7-TM, 7-transmembrane; ICL-3, 3<sup>rd</sup> intracellular loop; IP<sub>3</sub>, inositol 1,4,5-triphosphate; IP<sub>3</sub>R, inositol 1,4,5-triphosphate receptor; NE, norepinephrine; MOI, multiplicity of infection; MAPK, mitogen-activated protein kinase; cAMP, 3'-5'-cyclic adenosine monophosphate; HEK cells, human embryonic kidney cells; EBNA, Epstein-Barr nuclear antigen; NaBu, sodium butyrate; PLC, phospholipase C; DMSO, dimethyl sulfoxide; FLIPR, fluorometric imaging plate reader; HBSS, Hank's buffered salt solution; HEPES, 4-(2-hydroxyethyl)-1-piperazineethanesulfonic acid; BSA, bovine serum albumin; EPAC, exchange protein directly activated by cAMP; PKA, cAMP-dependent protein kinase; DAG, diacylglycerol; SERCA, sarco/endoplasmic reticulum  $Ca^{2+}$ -ATPase; FRET, Förster resonance energy transfer; AT1, Angiotensin II receptor type 1; ER, endoplasmic reticulum; TRP channel, transient receptor potential channel; ARC channel, arachidonate-regulated  $Ca^{2+}$ -selective channel; ERK, extracellular signal-regulated kinase; 2-APB, 2-Aminoethoxydiphenyl borate.

MOL #50765

## ABSTRACT

Agonist occupied  $\alpha_1$ -adrenoceptors ( $\alpha_1$ -AR) engage several signaling pathways including phosphatidylinositol hydrolysis, calcium mobilization, arachidonic acid release, MAP kinase activation and cAMP accumulation. The natural agonist norepinephrine (NE) activates with variable affinity and intrinsic efficacy all adrenoceptors and in cells such as cardiomyocytes that co-express  $\alpha_1$ - and  $\beta$ - AR subtypes, this leads to co-activation of multiple downstream pathways. This may result in pathway cross-talk with significant consequences to heart physiology and pathology. In order to dissect signaling components involved specifically in  $\alpha_{1A}$ - and  $\beta_2$ -AR signal interplay, we have developed a recombinant model system that mimics the levels of receptor expression observed in native cells. We followed intracellular  $\text{Ca}^{2+}$  mobilization to monitor in real time the activation of both  $G_q$  and  $G_s$  pathways. We found that co-activation of  $\alpha_{1A}$ - and  $\beta_2$ -AR by the non-selective agonist NE or via a combination of the highly selective  $\alpha_{1A}$ -AR agonist A61603 and the  $\beta$ -selective agonist isoproterenol led to increases in  $\text{Ca}^{2+}$  influx from the extracellular compartment relative to stimulation with A61603 alone, with no effect on the associated transient release of  $\text{Ca}^{2+}$  from intracellular stores. This effect became more evident upon examination of an  $\alpha_{1A}$ -AR variant exhibiting a partial defect in coupling to  $G_q$  and we attribute it to potentiation of a non  $G_q$ -pathway, uncovered by application of a combination of an endoplasmic reticulum  $\text{IP}_3$  receptor blocker, xestospongin C and the non-selective store-operated  $\text{Ca}^{2+}$  entry channel (SOC) blocker, 2APB. We also found that stimulation with A61603 of a second  $\alpha_{1A}$ -AR variant, entirely unable to signal did not induce any  $\text{Ca}^{2+}$  unless  $\beta_2$ - AR was concomitantly activated. These results may be accounted for by the presence of  $\alpha_{1A}/\beta_2$ -AR heterodimers or alternatively by specific adrenoceptor signal cross-talk resulting in distinct

MOL #50765

pharmacological behavior. Finally, our findings provide a new conceptual framework to rationalize outcomes from clinical studies targeting  $\alpha$ - and  $\beta$ -adrenoceptors.

MOL #50765

## INTRODUCTION

Given the diversity of physiological processes controlled by G protein-coupled receptors (GPCRs or 7-TM receptors) and the large number of receptors from this family co-expressed in different tissues, it comes as no surprise that linear signal transduction models cannot accommodate the many observed pharmacological outcomes that follow receptor activation. It is generally understood that intracellular signal transduction pathways stemming from the activation of GPCRs interact significantly to add layers of complexity to their regulation, sometimes leading to novel signaling modes (Cordeaux and Hill, 2002). Additionally, many receptors have been shown to couple to more than one G protein, and also initiate G protein-independent signaling upon stimulation (reviewed in Gilchrist, 2007; Violin and Lefkowitz, 2007).

Such GPCR signaling cross-talk can be initiated at the level of the receptor, via formation of heterodimers, or result from downstream integration of signals derived from other receptors with no physical association. For the adrenoceptor (AR) family, formation of functional homo and heterodimers is emerging as a common theme and its importance has been documented with multiple pharmacological observations (see review Prinster et al., 2005). Heterodimerization of  $\alpha_{1D}$ -AR with either  $\beta_2$ -AR or  $\alpha_{1B}$ -AR appears essential for its biogenesis and cell surface expression.  $\alpha_{1D}$ / $\alpha_{1B}$ -AR heterodimers also exhibit distinct ligand pharmacology and show enhanced agonist mediated activity, relative to either subtype alone. Many other heteroreceptor couplings have been reported to affect aspects of receptor function such as pharmacological behavior, internalization and desensitization, as well as differential signal transduction pathways. They include  $\alpha_{1A}$ / $\alpha_{1B}$ -,  $\beta_1$ / $\alpha_{2A}$ - and  $\beta_2$ / $\beta_1$ -AR (see review Prinster et al., 2005). Formation of heterodimers is not limited to within the adrenoceptor family members:

MOL #50765

adrenoceptors can also dimerize with opioid, muscarinic, histamine and olfactory GPCRs (reviewed in Prinster et al., 2005).

Signaling cross-talk may also result from the regulation of receptor function by accessory proteins or from the modification of the signaling properties of effector molecules by other elements of the activated pathway. Such interactions have been observed to increase or cross-inhibit responses, recruit cytoskeletal proteins, modulate channel activity or down-regulate receptor expression (reviewed in Hur and Kim, 2002; Werry et al., 2003). Pathway cross-talk has been introduced to describe inconsistent behavior of certain pharmacological agents such as  $\beta$ - and  $\alpha$ -AR agonists. Indeed, multiple studies have focused on the cardiac AR subtypes, particularly on interactions of  $\alpha_1$ - and  $\beta_1$ -AR agonists in the regulation of cardiac contractility and pace (reviewed in Dzimir, 2002). Much less is known with regard to interactions between  $\alpha_1$  and  $\beta_2$ -ARs, yet intriguing studies in aging and failing human hearts showed up-regulation of the expression of  $\alpha_{1A}$ -AR, with concomitant down-regulation of the  $\beta_1$ -AR, while  $\beta_2$ -AR expression levels remained unchanged (Woodcock et al., 2008). The resulting changes in the  $\alpha_1/\beta_2$  versus  $\beta_1$ -AR ratios suggest a crucial role for  $\alpha_1$ -AR in inotropic signaling and cytoprotection in the failing heart (Huang et al., 2007; Skomedal et al., 1997; Woodcock et al., 2008). At present, a framework for understanding the interplay between  $\alpha_1$  and  $\beta_2$ -adrenoceptors in intracellular signaling is lacking. Co-expression of  $\alpha_{1A}$ - and  $\beta_2$ -ARs in a model system was utilized for the functional dissection of cross-talk between those receptors, and in particular, one that allowed expression densities more closely matched to those seen in cardiomyocytes.

As part of our efforts to develop a SAR for selective  $\alpha_{1A}$ -AR agonists, we have identified receptor variants (at the level of the 3<sup>rd</sup> intracellular loop) that are defective for signaling through their canonical pathways. By taking advantage of the endogenous expression of  $\beta_2$ -AR in HEK-

MOL #50765

293 cells, we have developed a transient expression model system for  $\alpha_{1A}$ -AR, where this receptor is expressed at relatively low levels that are comparable to levels observed in native cells and tissues. We have used this system to monitor the kinetics of responses occurring within seconds upon agonist stimulation of  $\alpha_{1A}$ ,  $\beta_2$  or both adrenoceptors. Onset of calcium signals resulting from  $G_q$ -PLC-IP<sub>3</sub>R coupling is much faster relative to  $G_s$ -mediated responses, probably due to the previously reported lag time for cAMP accumulation (Lohse et al., 2008a). This temporal resolution of signals has allowed us to monitor in real-time  $G_q$  and  $G_s$  signals converging on  $Ca^{2+}$  mobilization. We have also used this model to study signaling-defective  $\alpha_{1A}$ -AR variants and detected strong potentiation of  $Ca^{2+}$  mobilization on co-stimulation of  $\alpha_{1A}$  and  $\beta_2$  adrenoceptors. Furthermore, the reconstitution of  $\alpha_{1A}$ -AR function by co-expression with  $\beta_2$ -AR suggests a direct interaction of these two receptors or convergence of downstream signaling pathways. These data may greatly help our understanding of the pathogenesis and progression of heart failure, and suggest approaches for therapeutic intervention.

MOL #50765

## MATERIAL AND METHODS

### *Materials and reagents*

Reagents were purchased from the following commercial suppliers: A61603, xamoterol, procaterol and fenoterol from Tocris (Ellisville, MO); norepinephrine, prazosin, phentolamine, ICI 118551, atenolol, salbutamol, propranolol, probenecid, BSA and glucose from Sigma-Aldrich (St. Luis, MO); isoproterenol and oxymetazoline from MP Biomedicals (Irvine, CA), sodium butyrate from Alfa Aesar (Ward Hill, MA); 2-APB from Calbiochem (San Diego, CA) and xestospongine C from Cayman Chemical (Ann Arbor, MI); HEPES, HBSS and Fluo3-AM from Invitrogen (Carlsbad, CA). [<sup>3</sup>H]-Prazosin and [<sup>125</sup>I]-CYP were purchased from Perkin Elmer (Boston, MA). Crude membranes were prepared from transduced or transfected HEK-293/EBNA cells as published (Vaughan et al., 1999) with one modification. Cells were resuspended in the lysis buffer without sucrose and broken using a Polytron homogenizer (3 x 30 s pulses).

### *Constructs*

The wild-type  $\alpha_{1A}$ -AR (WT- $\alpha_{1A}$ -AR) codon altered sequence was based on  $\alpha_{1A}$ -AR isoform 1 (Genbank NM\_000680). The full length gene was synthesized (DNA 2.0, Menlo Park) with an N-terminal HA tag (MVYPYDVPDYAGT), unique 5' - SacII and 3' - XhoI restriction sites flanking the region of the I3 loop to exchange CCPGCC (tetracysteine motif, TCM) I3 loop variants, a C-terminal 8X His tag followed by a Flag tag, and additional spacer amino acids followed by a stop codon (GSHHHHHHHHGSDYKDDDDKGGSTG-stop). This wild-type tagged  $\alpha_{1A}$ -AR gene was synthesized in a Gateway compatible plasmid and transferred by LR



MOL #50765

clonase reaction (Invitrogen, Carlsbad) into a high copy Gateway modified BacMam expression vector derived from pTriEx3 (EMD Biosciences, San Diego, CA).

For the insertion variant Ins\_ $\alpha_{1A}$ -AR, the TCM motif was placed between codons G244 and G245. For the substitution variant Sub\_ $\alpha_{1A}$ -AR, the TCM motif was replaced for the sequence DSEQVT133. Both variants were created by synthesizing I3 loop fragments containing the TCM motif CCPGCC flanked by SacII and XhoI restriction sites. To generate these variants, a codon altered wild-type  $\alpha_{1A}$ -AR Gateway-compatible construct was digested with SacII and XhoI and replaced with the insertion or substitution variant SacII-XhoI synthetic I3 loop fragment. These variants were then transferred by LR clonase into the high copy Gateway modified pTriEx3 expression vector.

The pTriEx recombinants were co-transfected along with the BD BaculoGold linearized baculovirus DNA (BD Biosciences, San Jose, CA) into Sf9 insect cells using Insect Gene Juice<sup>®</sup> (Novagen, Madison, WI) transfection reagent. Cells were incubated at 27 °C, with shaking for 7 days to allow generation of recombinant baculovirus (vTriEx). The virus containing supernatant was then harvested and infections of larger volume Sf9 cultures were performed to amplify virus stocks. Viruses were tittered and expression of receptor was verified by Western Blot, radioligand binding and antibody staining.

#### *Cell culture and transient transductions.*

Cell-based experiments were performed using suspension-adapted HEK-293/EBNA cells. These cells were grown in Free Style 293 media (Invitrogen) and maintained in a humidified incubator at 37 °C in 7% CO<sub>2</sub> with constant shaking at 150 rpm. Prior to experiments, cells were transduced with baculoviral strains harboring  $\alpha_{1A}$ -AR, aldehyde oxidase or viral medium

MOL #50765

(untransduced control). This was performed by incubating the cells with virus (MOI 100-150) for 3 to 4 h followed by exchange into fresh growth medium supplemented with 4 mM sodium butyrate (NaBu). Cells were grown for another 14 to 18 h, then examined for agonist-evoked responses in both intracellular  $\text{Ca}^{2+}$  mobilization and IP accumulation assays. Surface receptor density was determined by flow cytometry employing immunofluorescence labeling of the receptor's N-terminal hemagglutinin epitope tag and by radioligand binding using partially purified membranes.

#### *Ca<sup>2+</sup> mobilization FLIPR assay*

Virally transduced HEK-293/EBNA cells were resuspended in Hank's balanced salt solution w/o  $\text{Mg}^{2+}$ ,  $\text{Ca}^{2+}$  and phenol red (Invitrogen), supplemented with 2 mM  $\text{CaCl}_2$ , 10 mM HEPES pH 7.4, 2.5 mM probenecid, plus 1g/L each of glucose and BSA. Cells were then seeded in poly-D-lysine coated 96-well black plates with transparent bottom (Costar) at a density of 50,000 cells/well (0.1 mL volume). Cells were incubated for 1 h at 37 °C after addition of 0.1 mL of buffer supplemented with 4  $\mu\text{M}$  Fluo3-AM (1 mM stock solution prepared in 10% pluronic /DMSO and diluted to 4  $\mu\text{M}$  with loading buffer). Plates were then washed twice with 100  $\mu\text{L}$  of buffer and each well was refilled with 100  $\mu\text{L}$  of assay buffer. Agonist-evoked  $\text{Ca}^{2+}$  mobilization was monitored via FLIPR<sup>TM</sup> (MDS Analytical Technologies, Sunnyvale, CA). In experiments testing the effect of antagonist or inhibitor, 25  $\mu\text{L}$  of buffer were removed from the washed cells and 25  $\mu\text{L}$  of vehicle or test compound were added back to the wells, followed by incubation for the indicated times (typically 5-30 minutes) prior to measurement of agonist-evoked responses. A baseline fluorescence measurement (excitation 488 nm, emission 510–570 nm) was obtained, and responses to agonist were observed following addition of 50  $\mu\text{L}$ /well of agonist solution.

MOL #50765

Fluorescence (F) was measured for 1.5-2 min at 1 s intervals. All data were normalized to baseline fluorescence ( $F_0$ ) recorded 10 s prior to agonist addition and are represented as  $F/F_0$ , where  $F/F_0 = (F-F_0)/F_0 + 1$  at each time point.

### *IP Accumulation Assay*

Virally transduced HEK-293/EBNA cells were washed by centrifugation at 150 x g (8 min) and resuspended in the assay buffer (20 mM HEPES, 50 mM LiCl, 10 mM glucose, 1.8 mM  $\text{CaCl}_2$ , 0.5 mM  $\text{MgSO}_4$ , in HBSS 1X buffer) at a density of  $10^7$  cells/mL. Cells were dispensed in 10  $\mu\text{l}$  volume in 384-well black polystyrene plate (Costar) at  $10^5$ /well, and incubated with 10  $\mu\text{l}$  of antagonist or vehicle at room temperature. After 10 minutes, 10  $\mu\text{l}$  of agonist solution was added; incubations with agonist were varied from 5 to 30 minutes and stopped by addition of lysis buffer. Total inositol monophosphate (IP) was quantified using a homogeneous immunoassay method with time-resolved FRET detection (IP-One: Cisbio International, Bedford, MA), according to the instructions provided by the supplier. Fluorescence emission of the donor ( $\lambda = 620$  nm) and acceptor ( $\lambda = 665$  nm) were measured using a PHERAstar plate reader (BMG Labtech, Durham, NC). Triplicate samples were analyzed per data point and each experiment was performed independently at least two times.

### *Radioligand binding studies*

Ligand binding affinity was determined using membranes prepared from HEK-293/EBNA cells virally transduced or transiently transfected with  $\alpha_{1A}$ -AR constructs. [ $^3\text{H}$ ]-prazosin and [ $^{125}\text{I}$ ]-CYP were used as radioligands and 100  $\mu\text{M}$  phentolamine or 10  $\mu\text{M}$  propranolol as the respective non-radioactive competitors to determine non-specific binding. For competition

## MOL #50765

binding assays, unlabeled ligands (A61603, NE, and oxymetazoline) were used to compete [<sup>3</sup>H]-prazosin or [<sup>125</sup>I]-CYP binding. Reactions were set up in a 96-well polypropylene deep well-block (Beckman-coulter, Fullerton, CA) and initiated by the addition of 100 μL of membranes (5-40 μg of protein) to the mixture of radioligand and unlabeled competitor to give a final volume of 250 μL with buffer composition of 20 mM HEPES, 6 mM MgCl<sub>2</sub>, 1.4 mM EGTA, pH 7.4. The final concentrations of radioligands were 0.1-0.7 nM for [<sup>3</sup>H]-prazosin and 1 pM for [<sup>125</sup>I]-CYP. Plates were sealed with Parafilm and incubated for 90 min at 25°C. Reactions were terminated by rapid transfer to GF/B Unifilter-96 filter plates (PerkinElmer, Boston, MA) using a Filtermate 196 Harvester ( Packard Instrument, Downers Grove, IL), followed by two washes (1 mL each) with ice-cold 50 mM HEPES buffer (pH 7.4). UniFilters were dried in a fume hood for at least 1 h, and their backs were sealed with backing tape. 50 μl of MicroScint™-20 (PerkinElmer) was added to each well, and the plates were sealed with TopSeal-A (PerkinElmer). Filters were soaked overnight and the radioactivity counted using a TopCount microplate scintillation counter (Packard Instrument, Downers Grove, IL Packard Instrument, Hartford, CT). IC<sub>50</sub> values were estimated using the nonlinear least square fitting methods (GraphPad Prism, GraphPadSoftware, San Diego, CA) and pK<sub>i</sub> values were calculated according to the Cheng-Prusoff correction (Cheng and Prusoff, 1973).

### *Data Analysis*

Experiments were performed multiple times and carried out in replicates (n indicated in figure legends). Graphs shown reflect either pooled or representative data (see figure legends). For dose-response analysis, results from Ca<sup>2+</sup> mobilization experiments were plotted as peak F/F<sub>0</sub> vs. agonist concentration and fitted to a sigmoidal dose-response equation using the GraphPad Prism

MOL #50765

software package. For radioligand binding experiments,  $B_{\max}$  values were calculated from maximum binding using the equation  $B_{\max} = (SB \times (IC_{50} + [L])/[L])$ , where SB is the specific binding expressed as fmol per mg of membrane protein, and [L] is the ligand concentration.

MOL #50765

## RESULTS

### *Identification of $\alpha_{1A}$ -ARs displaying G protein coupling defects*

In generating probes to study GPCR conformational transitions that couple agonist binding to G protein activation via Förster resonance energy transfer (FRET), we prepared several mammalian cell expression constructs for fluorescent labeling, containing the arsenical-reactive tetracysteine motif (TCM, CCPGCC) (Hoffmann et al., 2005) in the third intracellular loop (ICL-3) of the  $\alpha_{1A}$ -AR, either as an insertion or a substitution. This strategy has been successfully applied to several receptors to observe ligand-induced conformational transitions leading to significant changes in the distance between the ICL-3 and the C-terminus of the receptor, thus changing FRET from the fluorescent probes placed at these two positions (Reviewed in Lohse et al., 2008b). The exact placement of TCM within ICL-3 was aimed at avoiding any impact on G protein coupling. Thus, amino acid positions found to participate in G protein coupling, or binding to scaffolding proteins, were avoided (Cotecchia et al., 1990; Greasley et al., 2001). Yet, two out of three variant receptors exhibited deficiencies in signaling. The insertion mutant Ins\_ $\alpha_{1A}$  AR displayed a partial coupling defect and the substitution mutant Sub\_ $\alpha_{1A}$  AR showed no functional coupling, as determined by their ability to produce inositol phosphates (IP) in response to NE stimulation (**Figure 1 A-D**). Treatment of cells expressing wild-type  $\alpha_{1A}$ -AR with the  $\alpha_{1A}$ -selective agonist A61603 or the native agonist NE induced similar levels of IP production at maximally effective agonist concentrations (**Figure 1A**). In both cases, EC<sub>50</sub> values were close to those previously reported for these agonists (NE: 0.9  $\mu$ M; A61603: 0.04  $\mu$ M. **Table 1**) (Ford et al., 1997). Cells bearing the variant Ins\_ $\alpha_{1A}$ -AR also showed similar rates of IP formation in response to both NE and A61603, yet those rates were lower relative to the ones observed in cells transduced with wild type\_ $\alpha_{1A}$ -AR, likely because of

MOL #50765

a decrease in signaling efficiency of that receptor variant (**Figure 1B**). A modest decrease in potency was detected in these cells for both agonists (NE: EC<sub>50</sub> = 4 μM; A61603: EC<sub>50</sub> = 0.2 μM. **Table 1**). No IP accumulation was detected with the Sub\_α<sub>1A</sub>-AR variant in response to NE or A61603 (**Figure 1C**). Finally, in untransduced HEK 293 cells treatment with these agonists resulted in no IP accumulation (**Figure 1D**). These results indicate a partially defective signaling phenotype for the insertion variant Ins\_α<sub>1A</sub> AR and complete impairment for the substitution variant Sub\_α<sub>1A</sub>-AR. Yet, Ins\_α<sub>1A</sub>-AR and Sub\_α<sub>1A</sub>-AR showed near-wild type binding properties for all ligands studied (**Table 2**), suggesting that their overall fold and structural stability is likely not affected by those modifications. Therefore, we considered these variants showing signaling defects to constitute useful tools for pharmacological studies aimed at dissecting the modes of signaling of α<sub>1A</sub>-ARs through downstream intracellular pathways.

### *A system to image adrenoceptor function using a Ca<sup>2+</sup> readout*

We studied these wild type and mutant α<sub>1A</sub>-AR baculovirus-delivered constructs based also on their ability to drive a fairly low level of surface receptor expression in most cells, as verified by antibody labeling and radioligand binding using crude membrane preparations (**Table 2** and Supplement **Figure S1A&B**) compared with the stably transfected CHO\_α<sub>1A</sub>-AR. Radioligand binding experiments indicate that expression levels were in the range of 400-650 femtomoles per milligram of membrane protein (**Table 2**), which is within two-fold of the determined expression levels of endogenous β<sub>2</sub>-AR (~300 fmol/mg) in these cells after butyrate treatment (**Table 2**). We found that both α<sub>1A</sub>- and β<sub>2</sub>-AR expression in these cells can be upregulated by addition of butyrate, a non-selective histone deacetylase inhibitor (Boffa et al., 1978). In naïve cells, this treatment seems to enhance signals from endogenous Ca<sup>2+</sup> channels in

MOL #50765

response to  $\beta_2$ -AR activation, providing us with a dynamic readout for the induction of cAMP or other mediators by following changes in  $\text{Ca}^{2+}$  mobilization not observed in untreated, parental HEK-293 cells. Thus, we have a cell-based system to monitor real-time signaling events involving  $\alpha_{1A}$  and  $\beta_2$  adrenoceptor activation, using fluorescence imaging of  $\text{Ca}^{2+}$  changes as a functional readout.

Incubation of untransduced, NaBu-treated cells with the non-selective adrenoceptor agonist NE induced a transient elevation of cytosolic  $\text{Ca}^{2+}$  (**Figure 2A**). The observed kinetics of the  $\text{Ca}^{2+}$  rise were relatively slow, with a consistent 10-second delay for the onset of the signal after agonist addition (**Figure 2A**, (+)). The maximal  $\text{Ca}^{2+}$  transient was observed within 40 seconds from NE addition, for most concentrations tested. This signal quickly decreased and did not trigger the activation of store-operated channels (SOCs) or any other  $\text{Ca}^{2+}$  re-entry mechanism, since the  $\text{Ca}^{2+}$  signal quickly returned to the basal level. We have tested several other  $\beta_2$ -AR selective and non-selective agonists such as fenoterol, procaterol, salbutamol and isoproterenol. All agonists examined evoked equivalent changes in intracellular  $\text{Ca}^{2+}$  release, with the expected rank order of potencies (**Figure 3A**). In contrast, the  $\beta_1$ -AR selective agonist xamoterol did not elicit any signals. Consistent with this, the observed agonist signals were sensitive to low concentrations (10 nM) of the  $\beta$ -AR selective antagonists propranolol (data not shown) and ICI 118,551 ( $\beta_2$ -selective), but not to the  $\alpha_1$ - selective antagonist prazosin (unpublished results) or the  $\beta_1$ -AR antagonist atenolol (**Figure 3B**). We did not detect any signals upon treatment of untransduced cells with the  $\alpha_{1A}$ -AR selective agonist A61603 (**Figure 2B**, (+)), confirming the absence of this receptor in the parental HEK-293 cells. NE induced  $\text{Ca}^{2+}$  mobilization in untransduced cells was sensitive to MDL12,330A and H89, the adenylate cyclase and PKA inhibitors, respectively suggesting that the observed changes in intracellular



MOL #50765

$\text{Ca}^{2+}$  are related to the activation  $G_s$  pathway (**Figure 3C**). Taken together, these results clearly indicate that the slow  $\text{Ca}^{2+}$  mobilization observed in naïve cells is derived from the activation of endogenous  $\beta_2$ -ARs. Consistent with this, the kinetics of the  $\text{Ca}^{2+}$  transient paralleled the dynamics of cAMP changes induced upon  $\beta_2$ -AR stimulation in these cells, as previously established using the cAMP sensor EPAC and cyclic nucleotide-gated channels as reporters (Violin et al., 2008).

The  $\text{Ca}^{2+}$  signaling properties of cells transduced with wild-type  $\alpha_{1A}$ -AR were clearly differentiated from untransduced controls. Upon addition of NE or the  $\alpha_{1A}$ -AR selective agonist A61603, we observed a fast increase in intracellular  $\text{Ca}^{2+}$  followed by a long-lasting (over several minutes, data not shown) sustained phase (**Figure 2 A&B**, (○)). The initial fast response is typical of  $G_q$ -mediated production of inositol 1,4,5-triphosphate ( $\text{IP}_3$ ), which in turn triggers the activation of the endoplasmic reticulum  $\text{IP}_3$  receptor ( $\text{IP}_3\text{R}$ ) and release of  $\text{Ca}^{2+}$  from that intracellular compartment (Reviewed in Clapham, 2007; Minneman, 1988). The ensuing sustained phase is presumed attributable to further mobilization of  $\text{Ca}^{2+}$  from the extracellular compartment, mediated by store-operated  $\text{Ca}^{2+}$  channels (Bugaj et al., 2005) as it is dependent upon presence of extracellular  $\text{Ca}^{2+}$  (data not shown). Although responses to both agonists appeared to be the same in their biphasic nature and kinetics of the initial calcium rise, closer inspection indicates noticeable differences in the temporal resolution of the transient phase between A61603 and NE-evoked signals. The transient response to NE appears to have a broader, longer lasting maximum relative to the one observed with the selective agonist A61603. The ratios of the transient peak response over the sustained phase are also noticeably different for these two  $\alpha_{1A}$ -AR agonists (1.2 for NE and 1.4 for A61603, at maximal response concentrations).

MOL #50765

### *Engineered $\alpha_{1A}$ -AR variants reveal signaling crossover with $\beta_2$ -ARs*

The observed differences in the temporal resolution of the transient phases of  $\text{Ca}^{2+}$  mobilization between NE and A61603 in wild type  $\alpha_{1A}$ -ARs were even more pronounced in cells expressing the partially active mutant Ins\_ $\alpha_{1A}$ -AR (**Figure 2 A&B**, (■)). In these cells, the initial  $\text{Ca}^{2+}$  rise reached maximum at a later time point for NE-evoked response (24 s) relative to A61603 (13 s), even though the NE peak was somewhat larger in amplitude (2.57 vs. 2.14). Stimulation of cells expressing the second variant, Sub\_ $\alpha_{1A}$ -AR, with NE produced a change in intracellular  $\text{Ca}^{2+}$  with a temporal resolution corresponding to the stimulation of endogenous  $\beta_2$ -AR, yet with significantly increased maximum response amplitude relative to untransduced cells (**Figure 2A**, (▲)). A61603 produced a very small and extremely slow increase in  $\text{Ca}^{2+}$  mobilization, manifesting a dramatic signaling deficiency in that modified receptor (**Figure 2B**, (▲)). Therefore, our findings with these variants confirm that NE stimulation of  $\alpha_{1A}$ -AR\_HEK-293 cells elicits a  $\text{Ca}^{2+}$  response comprising more than one phase, involving contributions from canonical  $\alpha_{1A}$ - and  $\beta_2$ -AR pathways, and seemingly non-canonical ones originating from these same receptors, yet to be resolved.

To examine the potency and response magnitude of the adrenoceptor agonists NE and A61603 in untransduced cells (**Figure 2C**) and cells transiently transduced with wild-type  $\alpha_{1A}$ -AR (**Figure 2D**) or the Ins\_ $\alpha_{1A}$ -AR (**Figure 2E**), we quantified the fast onset response peak amplitude ( $F/F_0$ ) of  $\text{Ca}^{2+}$  responses as a function of agonist concentration. The selective  $\alpha_{1A}$ -AR agonist A61603 produced dose-dependent  $\text{Ca}^{2+}$  responses only in  $\alpha_{1A}$ -AR transduced cells. The  $\text{EC}_{50}$  values were 3 nM for wild type  $\alpha_{1A}$ -AR and 6 nM for Ins- $\alpha_{1A}$ -AR (**Table 1**). This early peak was absent from the Sub\_ $\alpha_{1A}$ -AR calcium responses precluding determination of dose dependence correlation. As mentioned above, for the non-selective adrenoceptor agonist NE, the

MOL #50765

time course for  $\text{Ca}^{2+}$  transient responses is complex, making it difficult to isolate the effect of this ligand resulting solely from activation of  $\alpha_{1A}$ -AR cells. For this agonist peak responses occurred at 13 and 26 seconds from agonist addition, for wild type  $\alpha_{1A}$ -AR cells (apparent  $\text{EC}_{50}$  values of 70 nM) and Ins\_ $\alpha_{1A}$ -AR cells ( $\text{EC}_{50}$  = 130 nM), respectively (**Table 1**). Remarkably, even though NE and A61603 are both full agonists, A61603 showed only partial agonism relative to NE at the Ins\_ $\alpha_{1A}$ -AR variant, the only one amenable to quantification (**Table 1**). This differential signaling efficacy may account for the observed slow-down of the initial NE calcium peak, resulting in an overall transient that is shifted toward the maximum observed for the  $\beta_2$ -AR  $\text{Ca}^{2+}$  response. At a first approximation, this suggests a level of synergy in cross-talk between  $\alpha_{1A}$ - and  $\beta_2$ -adrenoceptors in this system as only NE will activate both subtypes. Yet, the activation of  $\beta_2$ -AR does not seem to change the response properties of  $\alpha_{1A}$ -AR at  $\text{G}_q$ , as both the selective and the non-selective agonists induced similar levels of IP accumulation (**Figure 1**), a more proximal readout for  $\text{G}_q$  coupling. Therefore, the observed higher efficacy of NE, as compared to A61603, to induce  $\text{Ca}^{2+}$ -mobilization in cells expressing Ins\_ $\alpha_{1A}$ -AR seems to reveal a component contributed by activation of endogenous  $\beta_2$ -ARs.

In order to resolve the contribution of the  $\beta_2$ -AR initiated signaling to the measured calcium mobilization, we studied the kinetics of response to NE and A61603 in the presence and absence of the  $\beta$ -selective antagonist propranolol at a saturating concentration (100 nM). Inhibition of the  $\beta_2$ -AR with propranolol eliminated the observed differences in the kinetics of NE versus A61603-induced  $\text{Ca}^{2+}$  mobilization in wild type  $\alpha_{1A}$ -AR-transduced cells (**Figure 4 A&B**). Thus,  $\beta$ -AR blockade made the NE  $\text{Ca}^{2+}$  response profile look similar to the one observed with A61603: a fast and transient peak of intracellular calcium followed by a long lasting, sustained phase. The ratio between the  $\text{Ca}^{2+}$  changes observed in the transient phase over the

MOL #50765

sustained phase (~ 1.4) and the kinetics of the initial  $\text{Ca}^{2+}$  rise were similar for both agonists in the presence of propranolol. The pharmacological behavior of the insertion ICL-3 variant was consistent with the following: the activation kinetics of cells expressing the partially active mutant Ins\_ $\alpha_{1A}$ -AR with either agonist in the presence of 100 nM propranolol was virtually identical to the one observed with wild-type  $\alpha_{1A}$ -AR cells, with smaller amplitudes for both the early calcium peak and the sustained phase (**Figure 4 C&D**). Responses of the Sub\_ $\alpha_{1A}$ -AR variant were almost entirely eliminated by addition of 100 nM propranolol. Only a minimal and extremely slow (over 100 s) increase in  $\text{Ca}^{2+}$  was detected, confirming our initial interpretation that this ICL-3 modification renders that  $\alpha_{1A}$ -AR variant incompetent for direct signaling (**Figure 4 C&D**). No responses could be detected in control untransduced cells pretreated with 100 nM propranolol (**Figure 4 C&D**).

#### *Effects of agonist occupancy at $\beta_2$ -ARs on the pharmacological behavior of $\alpha_{1A}$ -ARs*

In wild type  $\alpha_{1A}$ -AR cells, responses are primarily driven by the fast  $G_q$ -mediated release of  $\text{Ca}^{2+}$  from the endoplasmic reticulum. Therefore, the concentration-response to NE or A61603 that was derived from the magnitude of the initial phase of intracellular  $\text{Ca}^{2+}$  mobilization should not be affected by ligands acting at  $\beta_2$ -ARs. Indeed, we found that pre-incubation with propranolol had no significant effect on the dose-response curves of NE or A61603 (**Figure 4E**). However, in cells expressing variant  $\alpha_{1A}$  adrenoceptors the NE dose-response curve in the presence and absence of 100 nM propranolol revealed that this  $\beta$ -selective antagonist significantly decreased NE responses, with only a modest effect on the  $\text{EC}_{50}$  value (**Figure 4G**). In fact, for Ins\_ $\alpha_{1A}$ -AR transduced cells, the maximal response of NE in the presence of propranolol was equal to that of A61603, consistent with the contribution of  $\beta_2$ -AR to observed

MOL #50765

signals (**Figure 4G**). The lack of an effect of propranolol on the  $EC_{50}$  values of these agonists at  $\alpha_{1A}$ -AR transduced cells suggests that this  $\beta$ -selective AR antagonist either acts solely by blocking  $\beta$ -AR signaling or, alternatively, as a non-competitive antagonist at  $\alpha_{1A}$ -AR sites. We interpret these results as an indication that  $\beta_2$ -ARs require agonist occupancy and activation to exert an effect on  $\alpha_{1A}$ -AR initiated signaling. Additionally, the presence of antagonist-bound  $\beta_2$ -AR has no bearing on  $\alpha_{1A}$ -AR  $Ca^{2+}$  signaling. Thus, we did not see any evidence in this system for inverse agonism or  $\beta$ -adrenoceptor constitutive activity.

We also studied the effect of pre-treating transduced cells with the  $\alpha_{1A}$ -AR selective antagonist RS100329 (Williams et al., 1999) at a saturating concentration (100 nM). We observed rightward shifts for the  $EC_{50}$  values of both A61603 (3-800 nM at WT and 10-400 nM at Ins\_ $\alpha_{1A}$  AR) and NE (0.07-0.6  $\mu$ M at WT and 0.1-2  $\mu$ M at Ins\_ $\alpha_{1A}$  AR. **Figure 4 F&H**, closed vs. open symbols). Interestingly, this  $EC_{50}$  shift in the presence of RS100329 was more than one log greater for A61603 relative to NE, indicating that part of the response to NE alone is mediated via additional receptors to  $\alpha_{1A}$ -AR. The remaining activity that we observed with NE after treatment with RS100329 could be attributed to its action at  $\beta_2$ -ARs, unlikely to be antagonized by RS100329 at 100 nM (**Figure 4 F&H**). The antagonistic effect of RS100329 appeared to be partially insurmountable, probably due to incomplete achievement of equilibrium conditions (hemi-equilibrium condition) over the course of our  $Ca^{2+}$  recordings (Kenakin, 2004). Such pseudo-irreversible antagonism stems from the relatively slow rates of dissociation for antagonist relative to the short acquisition time of the experiment (Kenakin, 2004). This is also indicated by the  $Ca^{2+}$  mobilization profiles of wild-type  $\alpha_{1A}$ -AR cells pre-treated with RS100329, followed by stimulation with A61603: a slow, linear increase in  $Ca^{2+}$  was observed under those conditions (**Figure 4B**). Pre-treatment of those cells with RS100329, application of NE elicited a

MOL #50765

response with a 10-second delay in the  $\text{Ca}^{2+}$  rise (**Figure 4A**). The signals lacked any observable desensitization or rapid return to baseline. This may be due to slow recovery of  $\alpha_{1A}$ -AR signaling upon dissociation of RS100329 from the receptor, inherent to the non-equilibrium nature of transient measurements.

To further address whether activated  $\beta_2$ -ARs influence the signaling behavior of co-expressed  $\alpha_{1A}$ -ARs, we performed concentration-response analysis of A61603 and NE-mediated signaling in the presence or absence of a fixed concentration of the potent  $\beta$ -AR agonist isoproterenol (at  $\text{EC}_{75} \sim 10$  nM). NE is a fairly low affinity agonist at both  $\beta_2$ -AR and  $\alpha_{1A}$ -ARs (Perez, 2005), thus the level of both  $\alpha_{1A}$ -AR and  $\beta_2$ -AR activation should change with increasing concentrations of NE in  $\alpha_{1A}$ -AR transduced EBNA cells. We simplified our experimental system by keeping the occupancy (and activation) of  $\beta_2$ -ARs constant, by concomitant application of  $\alpha_{1A}$ -AR agonists and isoproterenol, assuming there is no influence of agonist occupancy at  $\alpha_{1A}$ -AR on that of the  $\beta_2$ -AR. As expected for untransduced cells, there were no responses to A61603 and only background responses to isoproterenol and NE were observed (**Figure 5A&E**). Simultaneous stimulation of wild-type  $\alpha_{1A}$ -AR cells with increasing concentrations of NE plus 10 nM isoproterenol resulted in dose-dependent increases in intracellular  $\text{Ca}^{2+}$  (**Figure 5B**). The  $\text{EC}_{50}$  was shifted to the left by roughly one log unit ( $\text{EC}_{50} = 0.008$   $\mu\text{M}$ ) relative to measurements in the absence of isoproterenol ( $\text{EC}_{50} = 0.06$   $\mu\text{M}$ ), indicating that this  $\beta$ -selective agonist acted as a potentiator of the  $\alpha_{1A}$ -AR response. The same effect was observed with A61603, although isoproterenol also increased the apparent maximum response to A61603 by about 20% ( $F/F_0 = 3.1$  and  $3.5$  at max. effective A61603). The observed increase in A61603 maximal effect in the presence of 10 nM isoproterenol became more evident in experiments employing cells expressing the  $\alpha_{1A}$ -AR ICL-3 variants (**Figure 5 C&D**). Because

MOL #50765

both mutants displayed a  $\text{Ca}^{2+}$  phase consistent with  $\beta_2$ -driven response (slow-rising peak with a maximum at 37 seconds post agonist addition), quantification of agonist potency and response amplitude was possible for Sub- $\alpha_{1A}$ -AR (**Figure 5 G&H**). 10 nM isoproterenol increased A61603 responses by 160% ( $F/F_0 = 1.8$  and  $3.1$ ) and 500% ( $F/F_0 = 1.1$  and  $1.9$ ) for the Ins- $\alpha_{1A}$ -AR and Sub- $\alpha_{1A}$ -AR cells, respectively (**Figure 5 C&D**). In all cases, the kinetics and amplitude of combined A61603 plus isoproterenol roughly equaled the response kinetics and amplitude of NE by itself (**Figure 5 F-H**).

More importantly, in the presence of 10 nM isoproterenol, A61603 induced a dose-dependent  $\text{Ca}^{2+}$  mobilization in cells expressing the coupling deficient Sub- $\alpha_{1A}$ -AR variant (**Figure 5D**). The observed  $\text{EC}_{50}$  value of 5 nM was comparable to the  $\text{EC}_{50}$  of A61603 alone at wild-type- $\alpha_{1A}$ -AR cells, and one log less potent than that observed for A61603 at wild type- $\alpha_{1A}$ -ARs in the presence of isoproterenol. This value is at least one thousand-fold more potent relative to the  $\text{EC}_{50}$  of A61603 at  $\beta_2$ -ARs. This suggests that the observed response occurs upon A61603 occupancy of Sub- $\alpha_{1A}$ -ARs only when  $\beta_2$ -ARs are simultaneously agonist activated. The necessity for  $\beta_2$ -AR activation is also evidenced by the time course of the induced  $\text{Ca}^{2+}$  rise, which clearly displays  $\beta_2$ -AR features: 10-second delay for the rise and return to baseline within the recording time window, consistent with receptor desensitization (**Figure 5H**). Thus, the isoproterenol-induced potentiation of the A61603-evoked calcium mobilization in Sub- $\alpha_{1A}$ -AR cells indicates that this variant, virtually devoid of signaling activity (no  $\text{Ca}^{2+}$  or IP response to A61603), was still able to interact with  $\beta_2$ -AR. As mentioned above, A61603 did not effect dose-dependent  $\text{Ca}^{2+}$  mobilization in untransduced cells, even in the presence of isoproterenol (**Figure 5A**). Therefore, this observation confirms that the response of Sub- $\alpha_{1A}$ -AR cells can not be a consequence of direct action of A61603 at  $\beta_2$ -AR.

MOL #50765

One way of rationalizing our results is to postulate the formation of  $\alpha_{1A}/\beta_2$ -AR heterodimers, where activation of the  $\beta_2$ -AR counterpart “rescues” the signaling capacity of the defective  $\alpha_{1A}$ -AR variant. It has been proposed that both GPCR homo and heterodimers can transactivate in a cooperative fashion to couple to associated G proteins (Carrillo et al., 2003). The ability of the selective  $\alpha_{1A}$  agonist A61603 to increase isoproterenol-mediated  $\beta_2$ -AR responses in cells expressing the signaling-defective mutant Sub- $\alpha_{1A}$ -AR is consistent with the concept of cooperative transactivation, where A61603-induced conformational changes in  $\alpha_{1A}$ -AR mediate the transactivation of the associated functional  $\beta_2$ -AR and its signaling. This is not surprising, since the position of the CCPGCC substitution in the ICL3 of this variant is likely to interfere with G protein-receptor interaction, but not with ligand binding or conformational transitions resulting from that event (see reviews Oldham and Hamm, 2007; Perez, 2007). As a corollary, the  $\beta$ -AR selective agonist isoproterenol induced downstream signaling from Sub- $\alpha_{1A}$ -AR, reflecting a non- $G_q$  coupling mode (see below). Therefore, this cooperative effect occurred in both directions.

### ***Contributions of cAMP-mediated signaling to the $\alpha_{1A}/\beta_2$ -AR cross-talk***

An alternate interpretation to the heterodimer hypothesis involves crossover of signals downstream from  $\alpha_{1A}$ - and  $\beta_2$ -ARs. To address this possibility, we used two different approaches. First, we asked whether the observed cross-talk was specific to  $\beta_2$ -AR signaling. For this, we examined the effects of forskolin, a direct activator of adenylyl cyclase that bypasses  $\beta_2$ -AR, and of NECA, an agonist of the  $G_s$ -coupled adenosine receptor 2B ( $A_{2B}$ ), endogenously expressed in HEK-293 cells (Cooper et al., 1997). Stimulation with 50  $\mu$ M forskolin or NECA in the absence of the  $\alpha_{1A}$ -AR agonist A61603 resulted in  $Ca^{2+}$  mobilization with similar temporal



MOL #50765

resolution to each other in both naïve and  $\alpha_{1A}$ -AR transduced cells (**Figure 6 A&C**). This validates the assumption that our experiments report on  $\text{Ca}^{2+}$  mobilization related to increases in intracellular cAMP. However, responses were much slower than the ones observed with  $\beta_2$ -AR agonists, reaching maximal levels only over 70 seconds from the time of compound addition. Those transients were also more persistent, suggesting a signaling mechanism less prone to desensitization. As expected, stimulation of naïve cells with increasing concentrations of A61603 in the absence or presence of 50  $\mu\text{M}$  forskolin or NECA did not result in a concentration-dependent, mobilization of calcium (**Figure 6B**). Stimulation of  $\alpha_{1A}$ -AR transduced cells with A61603 resulted in dose-dependent increases in intracellular calcium ( $\text{EC}_{50} = 3.1 \text{ nM}$ ) that were unaffected by co-stimulation with forskolin ( $\text{EC}_{50} = 1.4 \text{ nM}$ ) and only marginally potentiated by co-stimulation with NECA ( $\text{EC}_{50} = 0.9 \text{ nM}$ ; **Figure 6D**). Only NECA increased the response magnitude to A61603 modestly, by about 10%. Therefore, neither forskolin nor NECA recapitulated the calcium mobilization effects observed upon co-stimulation of cells with A61603 and isoproterenol.

Close examination of  $\text{Ca}^{2+}$  signal's time course indicates that both NECA and forskolin affected minimally the fast, transient phase (**Figure 6C**). Focusing on the sustained phase, forskolin appeared to elevate it with an apparent  $\text{Ca}^{2+}$  mobilization maximum at 50 s post compound addition. Surprisingly, while NECA had that same effect on the sustained phase, it also stimulated an additional component with intermediate kinetics relative to the fast and sustained phases (**Figure 6C**). Thus, even though NECA and forskolin contributed to A61603-induced signals from  $\alpha_{1A}$ -AR, the mechanism by which they mediate that effect seems to be different: there is no generic effector mechanism induced in these cells upon treatment with NaBu accounting for the  $\beta_2$ -AR effects observed on  $\alpha_{1A}$ -AR responses upon co-stimulation with

MOL #50765

A61603 and isoproterenol. Consistent with this interpretation, neither NECA nor forskolin recovered dose dependent transient responses to A61603 in the Sub- $\alpha_{1A}$  AR variant (**Figure 6F**). The dramatic functional rescue observed upon  $\beta_2$ -AR co-stimulation (**Figure 6E** gray vs solid red and green lines) was just not observed (**Figure 5 D&H**). As expected, the kinetics of those effects did not indicate recovery of  $G_q$  coupling (**Figure 6E**). As a corollary, the absence of functional rescue observed for this variant with either forskolin or NECA in the presence of NaBu further indicates that the pharmacological signatures that we observed are unequivocally dependent on  $\beta_2$ -AR signaling (**Figure 6 E&F** compared to **5 D&H**). Therefore, while these experiments indicate that certain aspects of the cross-talk such as potentiation of the sustained phase are directly correlated to generation of cAMP, they do not rule-out and actually support the presence of functional  $\alpha_{1A}/\beta_2$ -AR heterodimers.

### *Pharmacological dissection of $\alpha_{1A}$ -AR signaling events*

So far, our studies suggest the presence of an  $\alpha_{1A}$ -AR driven, non- $G_q$  signaling pathway that is potentiated by co-activation of  $\beta_2$ -AR. To isolate this component in our  $Ca^{2+}$  mobilization readout, we used a combination of xestospongine C and 2-APB, which are inhibitors of  $IP_3R$  and SOC channels, respectively. Therefore, this combination should remove from the  $Ca^{2+}$  transients any component of the signaling cascade initiated from  $G_q$  coupling. As suggested from previous results (**Figures 5F&6C**), wild type  $\alpha_{1A}$ -AR cells stimulated with NE or A61603 after pre-treatment with a combination of 5  $\mu M$  xestospongine C and 20  $\mu M$  2-APB exhibited a single phase of  $Ca^{2+}$  mobilization, devoid of both the rapid and sustained phases associated with  $G_q$  signaling (**Figure 7**, red and blue traces). Inclusion of 10 nM isoproterenol in addition to A61603 enhanced this “intermediate” response (**Figure 7**, dashed vs. solid blue lines). This

MOL #50765

phase had a maximum at 23 s post-agonist addition, about 10 s slower than the initial  $G_q$ -mediated response. (**Figure 7**, black dashed line). It became partly masked by the  $G_q$ -induced components observed in  $\alpha_{1A}$ -AR cells simultaneously stimulated with A61603 and isoproterenol in the absence of xestospongine C and 2-APB (**Figure 7**, black dashed line). These results indicate that additional, non-canonical signaling pathways contribute to intracellular  $Ca^{2+}$  mobilization. Thus, the observed intermediate component appears to be strongly tied to  $\beta_2$ -AR activation and apparently unrelated to  $G_q$  activation.

## DISCUSSION

In summary, here we present a broad range of internally consistent evidence for the functional interaction of  $\alpha_{1A}$ - and  $\beta_2$ -adrenoceptors. This provides a conceptual framework for previous pre-clinical and clinical findings suggesting such interactions. Furthermore, by using a well characterized cell-based model system allowing for manipulation of the expression levels of  $\alpha_{1A}$ - and  $\beta_2$ -ARs to mimic physiologically low expression levels, we were able to dissect the signaling components contributing to  $Ca^{2+}$  mobilization in response to activation of these two receptors. Relative to most transfection-based gene delivery methods, receptor expression driven by baculoviral gene transduction yields more homogeneous expression levels. This is indicated in FACS plots by the near-Gaussian distribution showing positive kurtosis (leptokurtic distribution) of  $\alpha_{1A}$ -AR transduced cells, where nearly 80% of them distribute within 3-fold from the geometric mean of the entire population (**Figure S1A**). At the same time, Figure S1A & B reveal small populations that display surface levels of  $\alpha_{1A}$ -AR expression above or below the bulk of the cells, which may introduce biases either to  $\beta_2$  or  $\alpha_{1A}$ -predominant functional readouts. Such small populations of untransduced cells expressing solely  $\beta_2$ -AR as well as  $\alpha_{1A}$ -AR over-

MOL #50765

expressing cells will always be present, yet they will likely lead to merely additive effects in measured  $\text{Ca}^{2+}$  mobilization, inconsistent with observations of non-additivity that we report here.

Figure 8 depicts in a diagrammatic, qualitative fashion the individual components that contribute to the  $\alpha_{1A}$ - and  $\beta_2$ -AR induced transients observed. The first, rapid transient phase peaking at ~12 seconds post-agonist addition reflects the activation of  $\text{IP}_3$ Rs and  $\text{Ca}^{2+}$  transfer from the ER to the cytoplasm (**Figure 8A**). The slower sustained phase depicted in **Figure 8B** represents entry of  $\text{Ca}^{2+}$  from the extracellular compartment after activation of CRAC or other reentry channels. The previously unidentified phase showing intermediate kinetics of  $\text{Ca}^{2+}$  mobilization (peaking at ~23 seconds post-agonist addition) is revealed only after inhibition of the contributions of  $\text{IP}_3$ Rs and calcium reentry channels. This component is likely to be mediated by cAMP through a  $G_q$ -dependent or independent mechanism (**Figure 8C**), although the precise identity of additional signaling components downstream from  $\beta_2$ -AR and the channel involved in this  $\text{Ca}^{2+}$  mobilization phase is yet to be identified. The  $\beta_2$ -AR signaling component is shown in **Figure 8D** as a delayed response peaking around 30 seconds, with appreciable desensitization thereof. Finally, the interplay of these phases is illustrated for cells transduced with wild type  $\alpha_{1A}$ -AR (**Figure 8E**) or the partially signaling-defective variant Ins\_ $\alpha_{1A}$ -AR (**Figure 8F**) on co-stimulation with the endogenously-expressed  $\beta_2$ -AR. These last two diagrams show how that potentiation of the intermediate phase by  $\beta_2$ -AR activation becomes apparent only with the partially active mutant, because of the decrease in the rapid transient and slow sustained phases. Although we attempted to build explicit models to account quantitatively for these phases, the inherent non-additivity of the effects observed upon receptor co-stimulation precluded construction of an adequate formal model.

MOL #50765

Our data show that  $\beta_2$ -AR activation can selectively influence the phases of  $\alpha_{1A}$ -AR induced  $\text{Ca}^{2+}$  mobilization, without affecting the rates of IP accumulation. Co-activation of  $\beta_2$ -AR, of adenylyl cyclase with forskolin, or stimulation of the  $G_s$ -coupled  $A_{2B}$  receptor with NECA has no effect on the first, rapid phase reflecting release of  $\text{Ca}^{2+}$  via  $\text{IP}_3\text{R}$  upon. Thus, it appears that an elevation in intracellular cAMP has no bearing on the activity of PLC and/or  $\text{IP}_3\text{R}$ . On the other hand, the sustained phase appeared to be uniformly potentiated by all three activation means, indicating a single mechanism for agonist-evoked calcium re-entry, either through capacitive  $\text{Ca}^{2+}$  release activated channels (CRAC), DAG-activated transient potential (TRP) channels, or through non-capacitive arachidonic acid-activated calcium channels (ARC) (Bugaj et al., 2005; Martin and Cooper, 2006; Mignen et al., 2005). The activity of the latter channel can be modulated via PKA phosphorylation mediated by A-kinase anchoring protein (AKAP) (Mignen et al., 2005).

Surprisingly, removal of the fast transient and slow sustained phases of  $\text{Ca}^{2+}$  mobilization in response to  $\alpha_{1A}$ -AR agonists, by application of selective blockers of the endoplasmic reticulum  $\text{IP}_3\text{R}$  and the plasma membrane SOCs, unmasked a distinct third phase. It could be argued that addition of xestospongine C simply delayed the  $\text{IP}_3$ -generated  $\text{Ca}^{2+}$  response. Thus, the third phase represents incomplete inhibition of  $\text{IP}_3\text{R}$ . Should that be the case, lower concentrations of xestospongine C would be expected to cause a lesser delay in  $\text{Ca}^{2+}$  mobilization. To address that possibility, we repeated this experiment at a lower concentration of xestospongine C and found that not to be the case; instead, the third phase remained insensitive to this  $\text{IP}_3\text{R}$  inhibitor, while the rapid  $\text{Ca}^{2+}$  mobilization phase reappeared, but at lower amplitude (data not shown). Therefore, instead of observing one single response phase with intermediate kinetics, we observed the two distinct and well-resolved phases illustrated in Figure 8 A&C.

MOL #50765

We do not know at present the identity of the channel responsible for the third phase (**Figure 8C**), nor the signaling cascade leading to its activation. In preliminary studies both adenylyl cyclase and PKA inhibitors fully blocked all responses, indicating the additional phase is also affected by cAMP signaling (data not shown). We also found that pretreatment with thapsigargin, a SERCA blocker, abolished all signals (data not shown). Therefore, the endoplasmic reticulum appears to be the likely source of  $\text{Ca}^{2+}$ . An alternate mechanism for the control of  $\text{Ca}^{2+}$  release from the ER involves ryanodine receptors (RyRs). They have been shown to exist in several non-excitabile cell lines, although their functional expression in HEK-293 cells is controversial. RT-PCR analysis of HEK-293/EBNA cells found that significant levels of RyR2 mRNA are present in these cells.

Both coupling deficient mutants are strongly potentiated by co-activation of  $\beta_2$ -AR. The Ins- $\alpha_{1A}$  AR mutant showed significantly higher potentiation relative to the wild-type receptor. This may indicate that the co-activation of wild-type  $\alpha_{1A}$ -AR with  $\beta_2$ -AR maximized the capacity for  $\text{Ca}^{2+}$  mobilization in those cells (response ceiling or saturation). Since the defective Ins- $\alpha_{1A}$ -AR mutant triggered a smaller increase in cytoplasmic  $\text{Ca}^{2+}$ , it likely allowed for greater potentiation by  $\beta_2$ -AR. Alternatively, higher concentrations of second messengers generated upon initial  $\alpha_{1A}$ -AR activation may interfere with the  $\beta_2$ -AR mediated potentiation effect. Either way, our findings suggest that in native tissues,  $\beta_2$ -AR may act as an amplifier of  $\alpha_{1A}$ -AR responses at “low”  $\alpha_{1A}$ -AR functional settings.

The most striking result was observed with the  $G_q$ -uncoupled Sub- $\alpha_{1A}$  AR mutant. Stimulation of cells expressing this variant with the  $\alpha_{1A}$ -selective agonist A61603 yielded no detectable  $\text{Ca}^{2+}$  mobilization or IP generation, yet this mutant showed recovery of  $\text{Ca}^{2+}$  mobilization in response to co-stimulation with the  $\beta_2$ -AR agonist isoproterenol and the  $\alpha_{1A}$ -AR

MOL #50765

agonist A61603. In those cells, A61603 increased  $\beta_2$ -AR activated  $\text{Ca}^{2+}$  mobilization in a concentration-dependent manner with an  $\text{EC}_{50}$  value consistent with the well documented activity of this compound at  $\alpha_{1A}$ -AR. These observations may indeed imply the formation of  $\alpha_{1A}/\beta_2$ -AR heterodimers in transduced cells though additional studies will be necessary to confirm this. Trans-activation, one of the proposed mechanisms of action for allosteric activation of GPCR heterodimers, provides a straightforward interpretation for the obtained results (Carrillo et al., 2003; Milligan and Smith, 2007).

An alternate interpretation not invoking heterodimers can also be put forward.  $\alpha_1$ -ARs have been found to activate multiple signaling pathways and to induce the generation of various second messengers depending on the agonist and cell line or tissue tested (reviewed in Perez, 2005). Still, little is known about the structural elements of the receptor involved in conferring functional selectivity, or the identity of any partner proteins. Thus, it is possible that the Sub\_  $\alpha_{1A}$  AR, even though uncoupled from  $\text{G}_q$ , may remain competent for induction of other signaling events that we have not probed. Moreover, activation of non- $\text{G}_q$  signaling cascades may remain subject to regulation of the Sub\_  $\alpha_{1A}$  AR cross-talk with  $\beta_2$ -AR. This would account for the observed increases in  $\beta_2$ -AR induced  $\text{Ca}^{2+}$ -mobilization on co-stimulation in Sub\_  $\alpha_{1A}$  AR cells. Another interpretation involves  $\beta_2$ -AR mediated sensitization of  $\alpha_{1A}$ -AR signaling; such a sensitizing effect may be revealed more clearly in the functionally impaired  $\alpha_{1A}$ -AR variants. While these alternative explanations remain plausible, the observed recovery of function observed with Sub\_  $\alpha_{1A}$  AR cells upon co-stimulation with A61603 and isoproterenol would seem to favor the  $\alpha_{1A}/\beta_2$ -AR heterodimer model.

Convergent regulation of  $\text{Ca}^{2+}$  channels involved in agonist-mediated  $\text{Ca}^{2+}$  mobilization provides another point of pathway intersection (Zamponi and Snutch, 2002). Multiple lines of

MOL #50765

evidence indicate that channel activity can be modulated by a variety of mechanisms including (1) phosphorylation by PKC, PKA, ERK and other kinases (Martin et al., 2006; Schulz et al., 2008), (2) modulation by interacting proteins such as calmodulin, AKAP, Snapin, G proteins ( $\beta$  subunits) or even receptors themselves (e.g.,  $\beta_2$ -AR with the L-type  $\text{Ca}^{2+}$  channel) (Catterall et al., 2006; Davare et al., 2001; Mignen et al., 2005; Suzuki et al., 2007) and (3) small molecule effectors (cAMP, cyclic ADP ribose,  $\text{IP}_3$ , arachidonic acid, diacylglycerol, etc.) (Berridge et al., 2003; Higashida et al., 2007; Hofmann et al., 1999; Mignen et al., 2005). Thus, co-activation of two cascades may lead to multiple effects converging on  $\text{Ca}^{2+}$  mobilization.

HEK-293 cells express markers common to cells of the neuronal lineage, including a wide variety of ligand- and voltage-gated calcium channels (Shaw et al., 2002). For several of them evidence of their expression includes electrophysiology studies as well as protein and mRNA readouts (Berjukow et al., 1996; Mignen et al., 2005). For the more extensively studied voltage gated  $\text{Ca}_v$  channels such as the L-type and N-type, it has been shown that they are subject to phosphorylation by PKA and PKC (Catterall et al., 2006; Kamp and Hell, 2000) while several putative phosphorylation sites have been identified in the T-type channels (Talavera and Nilius, 2006). Interestingly,  $\beta$ -adrenergic stimulation is one known mechanism of facilitation of the T-type currents. More recently,  $\text{Ca}_v$  channels have been reported to be regulated by the MAPK signaling cascade via ERK. Although ERK-dependent enhancement of  $\text{Ca}_v$  currents often is due to upregulation of the expression of these channels, the neuronal N-type channel may be ERK-phosphorylated and tonically stimulated by MAP kinases (Fitzgerald, 2002; Martin et al., 2006; Woodall et al., 2008). Therefore, activation of  $\alpha_{1A}$  and  $\beta_2$ -ARs could lead to simultaneous regulation of  $\text{Ca}_v$  via different mechanism, as has been demonstrated in cardiomyocytes expressing L-type channels (reviewed in Kamp and Hell, 2000).



MOL #50765

Recently, the expression of the  $\alpha_{1A}$  and  $\beta_2$ -ARs in myocardial tissue and their functional balance has been linked to the pathogenesis and progression of heart failure, implicating maladaptation of adrenoceptor signaling (Feldman et al., 2008; Huang et al., 2007; Woodcock et al., 2008). The development of heart failure in humans is accompanied by an increase in catecholamine levels, a decrease in density and signaling of the predominant adrenoceptor in the healthy heart,  $\beta_1$ -AR (Lohse et al., 2003), with no changes in the levels of expression of  $\beta_2$ -AR (Feldman et al., 2008; Woodcock et al., 2008). Since  $\alpha_{1A}$ -AR expression is maintained in heart failure, and the natural ligand norepinephrine is shared by both  $\alpha$ - and  $\beta$ -adrenoceptors,  $\alpha_{1A}$  and  $\beta_2$ -adrenoceptors are suggested to play greater roles in maintaining cardiac performance in failing hearts (Brodde, 1991; Skomedal et al., 1997; Woodcock et al., 2008).

Multiple lines of pre-clinical and clinical evidence suggest that a balance between  $\beta$ -ARs and  $\alpha_1$ -ARs signaling is critical for cardiomyocyte function and survival and may not necessarily involve the canonical pathways. In a transgenic mouse model, over-expression of  $G_q$  induces cardiac hypertrophy, loss of  $\beta$ -AR inotropic responsiveness (D'Angelo et al., 1997) and ultimately leads to heart failure (Sakata et al., 1998). On the other hand,  $\alpha_{1A/1B}$  double KO mice also developed heart failure after transverse aortic constriction and reconstitution of  $\alpha_{1A}$  signaling in cardiomyocytes from those animals rescued them from NE-induced apoptosis (O'Connell et al., 2006). Unexpectedly, no IP generation was detectable on those cardiomyocytes with reconstituted  $\alpha_{1A}$ -AR function or in wild type mouse cardiomyocytes, pointing at a non- $G_q$  signaling mode for this receptor in myocardial function. Recently, Simpson and coworkers have reported that  $\alpha_{1A}$ -AR stimulation of an ERK-mediated pathway is critical for cardiomyocyte survival (Huang et al., 2007).

MOL #50765

Seemingly contradicting clinical trial outcomes can actually be reconciled through this concept of  $\alpha_1/\beta$ -AR balanced pharmacology in the heart: while the selective  $\alpha_1$ -AR antagonist doxazosin worsened heart failure symptoms and increased mortality in heart failure patients, the non-selective antagonist carvedilol has shown efficacious in the treatment of this condition, and it is perhaps the most efficacious  $\beta$ -blocker in the clinic (ALLHAT, 2000; Metra et al., 2000). Thus, identifying the functional relationships between  $\beta_2$ - and  $\alpha_{1A}$ -ARs may be critical for understanding the pathophysiology of the failing heart, and for identifying further therapies.

Toward that goal, we have studied the cross-talk between  $\alpha_{1A}$ - and  $\beta_2$ -AR pathways employing a real-time functional readout combined with pharmacological analysis. Receptor cross-talk remains challenging to study at the cellular level, and native cellular models often display undetectable or altered receptor function, as a result of cell isolation and culturing prior to experimentation. On the other hand, studies employing systems relying on recombinant receptor expression commonly suffer from receptor over-production, leading to experimental artifacts. Thus, our approach was to take advantage of the well characterized HEK-293 cell line, which endogenously expresses  $\beta_2$ -AR, by introducing  $\alpha_{1A}$ -AR at low, and thus more physiological, expression levels. We employed the non-selective histone deacetylase inhibitor sodium butyrate to fine-tune receptor expression to levels comparable to the ones observed in native adrenergic tissues, as measured by radioligand binding. This system allowed us to measure in real-time adrenoceptor signaling via  $\text{Ca}^{2+}$  measurements derived from single or combined  $\alpha_{1A}$ - and  $\beta_2$ -AR activation. Our data provide for the first time detailed information on bidirectional cross-talk between  $\alpha_{1A}$ - and  $\beta_2$ -adrenoceptors. Surprisingly, they indicate that their functional interaction involves either heterodimer formation and/or the presence of yet to be identified  $G_q$  or non- $G_q$  signaling events in response to  $\alpha_{1A}$ -AR activation. Neither of those

MOL #50765

possibilities has been considered before to account for the physiological observations suggesting cross-talk between these two receptors. Dissection of the precise interplay of those signaling pathways in normal and diseased heart tissue, and in response to pharmacological agents, is the obvious follow-up to our studies. Such future study offers great potential for developing safer and more efficacious drugs for the treatment of heart failure and related conditions.

### **ACKNOWLEDGMENTS**

We are grateful to the Discovery Technologies Group of Roche Palo Alto: Michelle Browner and Tom Novak for their critical support to enable this work, Pamela Olson, Simon Lee, Mariola Ilnicka and Nixy Zutshi for help or expert advice. We also thank members of the *In Vitro* Pharmacology Group-Inflammation Discovery.

MOL #50765

## REFERENCES

- ALLHAT (2000) Major cardiovascular events in hypertensive patients randomized to doxazosin vs chlorthalidone: the antihypertensive and lipid-lowering treatment to prevent heart attack trial (ALLHAT). ALLHAT Collaborative Research Group. *Jama* **283**(15):1967-1975.
- Berjukow S, Doring F, Froschmayr M, Grabner M, Glossmann H and Hering S (1996) Endogenous calcium channels in human embryonic kidney (HEK293) cells. *British journal of pharmacology* **118**(3):748-754.
- Berridge MJ, Bootman MD and Roderick HL (2003) Calcium signalling: dynamics, homeostasis and remodelling. *Nature reviews* **4**(7):517-529.
- Boffa LC, Vidali G, Mann RS and Allfrey VG (1978) Suppression of histone deacetylation in vivo and in vitro by sodium butyrate. *The Journal of biological chemistry* **253**(10):3364-3366.
- Brodde OE (1991) Beta 1- and beta 2-adrenoceptors in the human heart: properties, function, and alterations in chronic heart failure. *Pharmacological reviews* **43**(2):203-242.
- Bugaj V, Alexeenko V, Zubov A, Glushankova L, Nikolaev A, Wang Z, Kaznacheyeva E, Bezprozvanny I and Mozhayeva GN (2005) Functional properties of endogenous receptor- and store-operated calcium influx channels in HEK293 cells. *The Journal of biological chemistry* **280**(17):16790-16797.
- Carrillo JJ, Pediani J and Milligan G (2003) Dimers of class A G protein-coupled receptors function via agonist-mediated trans-activation of associated G proteins. *The Journal of biological chemistry* **278**(43):42578-42587.
- Catterall WA, Hulme JT, Jiang X and Few WP (2006) Regulation of sodium and calcium channels by signaling complexes. *Journal of receptor and signal transduction research* **26**(5-6):577-598.
- Cheng Y and Prusoff WH (1973) Relationship between the inhibition constant (K<sub>1</sub>) and the concentration of inhibitor which causes 50 per cent inhibition (I<sub>50</sub>) of an enzymatic reaction. *Biochemical pharmacology* **22**(23):3099-3108.
- Clapham DE (2007) Calcium signaling. *Cell* **131**(6):1047-1058.
- Cooper J, Hill SJ and Alexander SP (1997) An endogenous A<sub>2</sub>B adenosine receptor coupled to cyclic AMP generation in human embryonic kidney (HEK 293) cells. *British journal of pharmacology* **122**(3):546-550.
- Cordeaux Y and Hill SJ (2002) Mechanisms of cross-talk between G-protein-coupled receptors. *Neuro-Signals* **11**(1):45-57.

MOL #50765

- Cotecchia S, Exum S, Caron MG and Lefkowitz RJ (1990) Regions of the alpha 1-adrenergic receptor involved in coupling to phosphatidylinositol hydrolysis and enhanced sensitivity of biological function. *Proceedings of the National Academy of Sciences of the United States of America* **87**(8):2896-2900.
- D'Angelo DD, Sakata Y, Lorenz JN, Boivin GP, Walsh RA, Liggett SB and Dorn GW, 2nd (1997) Transgenic Galphaq overexpression induces cardiac contractile failure in mice. *Proceedings of the National Academy of Sciences of the United States of America* **94**(15):8121-8126.
- Davare MA, Avdonin V, Hall DD, Peden EM, Burette A, Weinberg RJ, Horne MC, Hoshi T and Hell JW (2001) A beta2 adrenergic receptor signaling complex assembled with the Ca<sup>2+</sup> channel Cav1.2. *Science (New York, NY)* **293**(5527):98-101.
- Dzimiri N (2002) Receptor crosstalk. Implications for cardiovascular function, disease and therapy. *European journal of biochemistry / FEBS* **269**(19):4713-4730.
- Feldman DS, Elton TS, Sun B, Martin MM and Ziolo MT (2008) Mechanisms of Disease: detrimental adrenergic signaling in acute decompensated heart failure. *Nature clinical practice*.
- Fitzgerald EM (2002) The presence of Ca<sup>2+</sup> channel beta subunit is required for mitogen-activated protein kinase (MAPK)-dependent modulation of alpha1B Ca<sup>2+</sup> channels in COS-7 cells. *The Journal of physiology* **543**(Pt 2):425-437.
- Ford AP, Daniels DV, Chang DJ, Gever JR, Jasper JR, Lesnick JD and Clarke DE (1997) Pharmacological pleiotropism of the human recombinant alpha1A-adrenoceptor: implications for alpha1-adrenoceptor classification. *British journal of pharmacology* **121**(6):1127-1135.
- Gilchrist A (2007) Modulating G-protein-coupled receptors: from traditional pharmacology to allosterics. *Trends in pharmacological sciences* **28**(8):431-437.
- Greasley PJ, Fanelli F, Scheer A, Abuin L, Nenniger-Tosato M, DeBenedetti PG and Cotecchia S (2001) Mutational and computational analysis of the alpha(1b)-adrenergic receptor. Involvement of basic and hydrophobic residues in receptor activation and G protein coupling. *The Journal of biological chemistry* **276**(49):46485-46494.
- Higashida H, Salmina AB, Olovyannikova RY, Hashii M, Yokoyama S, Koizumi K, Jin D, Liu HX, Lopatina O, Amina S, Islam MS, Huang JJ and Noda M (2007) Cyclic ADP-ribose as a universal calcium signal molecule in the nervous system. *Neurochemistry international* **51**(2-4):192-199.
- Hoffmann C, Gaietta G, Bunemann M, Adams SR, Oberdorff-Maass S, Behr B, Vilardaga JP, Tsien RY, Ellisman MH and Lohse MJ (2005) A FIAsh-based FRET approach to

MOL #50765

- determine G protein-coupled receptor activation in living cells. *Nature methods* **2**(3):171-176.
- Hofmann T, Obukhov AG, Schaefer M, Harteneck C, Gudermann T and Schultz G (1999) Direct activation of human TRPC6 and TRPC3 channels by diacylglycerol. *Nature* **397**(6716):259-263.
- Huang Y, Wright CD, Merkwang CL, Baye NL, Liang Q, Simpson PC and O'Connell TD (2007) An alpha1A-adrenergic-extracellular signal-regulated kinase survival signaling pathway in cardiac myocytes. *Circulation* **115**(6):763-772.
- Hur EM and Kim KT (2002) G protein-coupled receptor signalling and cross-talk: achieving rapidity and specificity. *Cellular signalling* **14**(5):397-405.
- Kamp TJ and Hell JW (2000) Regulation of cardiac L-type calcium channels by protein kinase A and protein kinase C. *Circulation research* **87**(12):1095-1102.
- Kenakin TP (2004) *A pharmacology primer : theory, application and methods*. Elsevier, Amsterdam ; Boston.
- Lohse MJ, Engelhardt S and Eschenhagen T (2003) What is the role of beta-adrenergic signaling in heart failure? *Circulation research* **93**(10):896-906.
- Lohse MJ, Hein P, Hoffmann C, Nikolaev VO, Vilaradaga JP and Bunemann M (2008a) Kinetics of G-protein-coupled receptor signals in intact cells. *British journal of pharmacology* **153** Suppl 1:S125-132.
- Lohse MJ, Nikolaev VO, Hein P, Hoffmann C, Vilaradaga JP and Bunemann M (2008b) Optical techniques to analyze real-time activation and signaling of G-protein-coupled receptors. *Trends in pharmacological sciences* **29**(3):159-165.
- Martin AC and Cooper DM (2006) Capacitative and 1-oleyl-2-acetyl-sn-glycerol-activated Ca(2+) entry distinguished using adenylyl cyclase type 8. *Molecular pharmacology* **70**(2):769-777.
- Martin SW, Butcher AJ, Berrow NS, Richards MW, Paddon RE, Turner DJ, Dolphin AC, Sihra TS and Fitzgerald EM (2006) Phosphorylation sites on calcium channel alpha1 and beta subunits regulate ERK-dependent modulation of neuronal N-type calcium channels. *Cell calcium* **39**(3):275-292.
- Metra M, Giubbini R, Nodari S, Boldi E, Modena MG and Dei Cas L (2000) Differential effects of beta-blockers in patients with heart failure: A prospective, randomized, double-blind comparison of the long-term effects of metoprolol versus carvedilol. *Circulation* **102**(5):546-551.

MOL #50765

- Mignen O, Thompson JL and Shuttleworth TJ (2005) Arachidonate-regulated Ca<sup>2+</sup>-selective (ARC) channel activity is modulated by phosphorylation and involves an A-kinase anchoring protein. *The Journal of physiology* **567**(Pt 3):787-798.
- Milligan G and Smith NJ (2007) Allosteric modulation of heterodimeric G-protein-coupled receptors. *Trends in pharmacological sciences* **28**(12):615-620.
- Minneman KP (1988) Alpha 1-adrenergic receptor subtypes, inositol phosphates, and sources of cell Ca<sup>2+</sup>. *Pharmacological reviews* **40**(2):87-119.
- O'Connell TD, Swigart PM, Rodrigo MC, Ishizaka S, Joho S, Turnbull L, Tecott LH, Baker AJ, Foster E, Grossman W and Simpson PC (2006) Alpha1-adrenergic receptors prevent a maladaptive cardiac response to pressure overload. *The Journal of clinical investigation* **116**(4):1005-1015.
- Oldham WM and Hamm HE (2007) How do receptors activate G proteins? *Advances in protein chemistry* **74**:67-93.
- Perez DM (2005) *The adrenergic receptors : in the 21st century*. Humana Press, Totowa, N.J.
- Perez DM (2007) Structure-function of alpha1-adrenergic receptors. *Biochemical pharmacology* **73**(8):1051-1062.
- Prinster SC, Hague C and Hall RA (2005) Heterodimerization of g protein-coupled receptors: specificity and functional significance. *Pharmacological reviews* **57**(3):289-298.
- Sakata Y, Hoit BD, Liggett SB, Walsh RA and Dorn GW, 2nd (1998) Decomensation of pressure-overload hypertrophy in G alpha q-overexpressing mice. *Circulation* **97**(15):1488-1495.
- Schulz DJ, Temporal S, Barry DM and Garcia ML (2008) Mechanisms of voltage-gated ion channel regulation: from gene expression to localization. *Cell Mol Life Sci* **65**(14):2215-2231.
- Shaw G, Morse S, Ararat M and Graham FL (2002) Preferential transformation of human neuronal cells by human adenoviruses and the origin of HEK 293 cells. *Faseb J* **16**(8):869-871.
- Skomedal T, Borthne K, Aass H, Geiran O and Osnes JB (1997) Comparison between alpha-1 adrenoceptor-mediated and beta adrenoceptor-mediated inotropic components elicited by norepinephrine in failing human ventricular muscle. *The Journal of pharmacology and experimental therapeutics* **280**(2):721-729.
- Suzuki F, Morishima S, Tanaka T and Muramatsu I (2007) Snapin, a new regulator of receptor signaling, augments alpha1A-adrenoceptor-operated calcium influx through TRPC6. *The Journal of biological chemistry* **282**(40):29563-29573.

MOL #50765

- Talavera K and Nilius B (2006) Biophysics and structure-function relationship of T-type Ca<sup>2+</sup> channels. *Cell calcium* **40**(2):97-114.
- Violin JD, DiPilato LM, Yildirim N, Elston TC, Zhang J and Lefkowitz RJ (2008) beta2-adrenergic receptor signaling and desensitization elucidated by quantitative modeling of real time cAMP dynamics. *The Journal of biological chemistry* **283**(5):2949-2961.
- Violin JD and Lefkowitz RJ (2007) Beta-arrestin-biased ligands at seven-transmembrane receptors. *Trends in pharmacological sciences* **28**(8):416-422.
- Waugh DJ, Gaivin RJ, Damron DS, Murray PA and Perez DM (1999) Binding, partial agonism, and potentiation of alpha(1)-adrenergic receptor function by benzodiazepines: A potential site of allosteric modulation. *The Journal of pharmacology and experimental therapeutics* **291**(3):1164-1171.
- Werry TD, Wilkinson GF and Willars GB (2003) Mechanisms of cross-talk between G-protein-coupled receptors resulting in enhanced release of intracellular Ca<sup>2+</sup>. *The Biochemical journal* **374**(Pt 2):281-296.
- Williams TJ, Blue DR, Daniels DV, Davis B, Elworthy T, Gever JR, Kava MS, Morgans D, Padilla F, Tassa S, Vimont RL, Chapple CR, Chess-Williams R, Eglen RM, Clarke DE and Ford AP (1999) In vitro alpha1-adrenoceptor pharmacology of Ro 70-0004 and RS-100329, novel alpha1A-adrenoceptor selective antagonists. *British journal of pharmacology* **127**(1):252-258.
- Woodall AJ, Richards MA, Turner DJ and Fitzgerald EM (2008) Growth factors differentially regulate neuronal Cav channels via ERK-dependent signalling. *Cell calcium* **43**(6):562-575.
- Woodcock EA, Du XJ, Reichelt ME and Graham RM (2008) Cardiac alpha 1-adrenergic drive in pathological remodelling. *Cardiovascular research* **77**(3):452-462.
- Zamponi GW and Snutch TP (2002) Modulating modulation: crosstalk between regulatory pathways of presynaptic calcium channels. *Molecular interventions* **2**(8):476-478.



MOL #50765

## LEGENDS FOR FIGURES

**Figure 1.** Inositol phosphate accumulation following stimulation of transduced or untransduced HEK-293/EBNA cells with NE or A61603.

HEK-293/EBNA cells transduced with baculovirus strains carrying wild-type (**A**), Ins\_ $\alpha_{1A}$ -AR (**B**) or Sub\_ $\alpha_{1A}$ -AR (**C**) along with parental control cells (**D**) were pre-treated with NaBu for 18 hours to induce receptor expression. Cells were then plated and NE (●) or A61603 (■) was applied for 20 min, followed by termination of reaction with lysis buffer and quantification of IP. A representative experiment is shown, where each data point is the average value of triplicate samples.

**Figure 2.** Ca<sup>2+</sup> mobilization in transduced HEK-293/EBNA cells upon stimulation with norepinephrine (NE) or A61603.

Cells were transduced with baculoviral strains carrying control, wild-type  $\alpha_{1A}$ -AR and ICL3 variants Ins\_ $\alpha_{1A}$ -AR or Sub\_ $\alpha_{1A}$ -AR, followed by treated with NaBu for 18 hours prior to experiments. Cells were then dispensed into 96-well plates and loaded with fluorescent dye. Ca<sup>2+</sup> transients in response to stimulation with NE or A61603 were monitored fluorometrically.

**Panels A and B:** normalized, time-dependent changes after treatment with 1  $\mu$ M NE and 100 nM A61603, respectively. Untransduced control (+), wild-type  $\alpha_{1A}$ -AR (○) and ICL3 variants Ins\_ $\alpha_{1A}$ -AR (■) and Sub\_ $\alpha_{1A}$ -AR (▲). Arrow at 10 s indicates time of agonist addition. **Panels C-E:** concentration-effect curves for NE (●) or A61603 (■) mediated Ca<sup>2+</sup> transient responses in untransduced cells (**C**) or cells transduced with wild-type (**D**) and Ins\_ $\alpha_{1A}$ -AR (**E**). Data points represent peak fluorescence values of the recorded Ca<sup>2+</sup> transients in response to agonist addition

MOL #50765

and are reported relative to baseline values measured 10 s pre-addition. Each experiment was performed three independent times, with duplicates.

**Figure 3.** Ca<sup>2+</sup> mobilization in untransduced, NaBu-treated HEK-293/EBNA cells upon stimulation with  $\beta$ -AR agonist.

HEK-293/EBNA cells were treated with NaBu for 18 hours prior to experiments. Cells were then plated on 96-well plates, loaded with fluorescent dye (*Materials and Methods*) and washed. **A:** Left panel: Cells were treated with increasing concentrations of procaterol (■), xamoterol (○), salbutamol (▼), fenoterol (△) or isoproterenol (◆). Right panel: Kinetics of Ca<sup>2+</sup> mobilization at in the same cells treated with 3  $\mu$ M of procaterol (solid grey line), salbutamol (dashed grey line), fenoterol (solid black line) or isoproterenol (dashed black line). **B:** A second set of cells was pretreated with vehicle (■), 10 nM ICI119551 (△) or 1  $\mu$ M atenolol (○) for 5 min and stimulated with increasing doses of NE (Left panel), isoproterenol (Center panel) or fenoterol (Right panel). **C:** Cells were pretreated with vehicle (solid black line), 25  $\mu$ M of MDL12,330A (left panel, dashed, black line) or H89 (right panel, dashed, black line) for 30 min and stimulated with 1  $\mu$ M of NE. Changes in cytoplasmic Ca<sup>2+</sup> levels were monitored by fluorometry. Changes in cytoplasmic Ca<sup>2+</sup> levels were monitored by fluorometry. Data points represent peak fluorescence values of the recorded Ca<sup>2+</sup> transients in response to agonist addition and are reported relative to baseline values measured 10 s pre-addition. Each experiment was performed two independent times, with duplicates.

MOL #50765

**Figure 4.**  $\text{Ca}^{2+}$  mobilization in transduced HEK-293/EBNA cells upon stimulation with NE or A61603 in presence of  $\alpha_{1A}$ - and  $\beta$ -AR selective antagonists.

Cells were transduced with baculovirus stocks encoding wild-type or the ICL3  $\alpha_{1A}$ -AR variants, followed by 18 hours treatment with NaBu and measurement of  $\text{Ca}^{2+}$  transient response. **Panels**

**A-B:** Fluorescence changes relative to baseline ( $F/F_0$ ) in wild-type  $\alpha_{1A}$ -AR\_HEK-293/EBNA cells pre-treated for 10 min with vehicle ( $\blacktriangle$ ), 10 nM propranolol ( $\square$ ) or 10 nM RS100329 ( $\circ$ ), followed by stimulation with 1  $\mu\text{M}$  NE (**A**) or 100 nM A61603 (**B**). Arrows indicate the time of agonist addition. **Panels C-D:** Kinetics of NE (**C**) or A61603 (**D**) induced  $\text{Ca}^{2+}$  mobilization observed in HEK-293/EBNA cells transduced with control ( $\triangle$ ), wild-type ( $\circ$ ), Ins\_ $\alpha_{1A}$ -AR ( $\diamond$ ) or Sub\_ $\alpha_{1A}$ -AR ( $\square$ ) baculoviral strains following propranolol pre-treatment (10 nM, 10 min) of

**Panels E-H:** Cells expressing wild-type  $\alpha_{1A}$ -AR (**E&F**) or Ins\_ $\alpha_{1A}$ -AR (**G&H**) were pretreated with either 100 nM propranolol (**E&G**, open symbols), or 10 nM RS100329 (**F&H**, open symbols), followed by incubation for 5 minutes. Each plate also contained control wells with cells that were pretreated with vehicle under the same conditions (E-H, filled symbols).

Concentration-effect curves of A61603 ( $\blacksquare$ ,  $\square$ ) or NE ( $\bullet$ ,  $\circ$ )-mediated  $\text{Ca}^{2+}$  transient responses were determined from peak fluorescence relative to baseline ( $F/F_0$ ), plotted against agonist concentration. Data points are representative of three independent measurements with duplicate (controls) or triplicate (agonist-treated) samples. Data points reflect the average values of duplicate samples.

**Figure 5.** Potentiation of the agonist-evoked rise in cytoplasmic  $\text{Ca}^{2+}$  by 10 nM isoproterenol. HEK-293/EBNA cells were transduced with control (**A, E**), wild-type (**B, F**), Ins\_ $\alpha_{1A}$ -AR (**C, G**) or Sub\_ $\alpha_{1A}$ -AR (**D, H**) baculoviral strains, followed by 18 hours treatment with NaBu and

MOL #50765

measurement of  $\text{Ca}^{2+}$  transient response. **Panels A-D:** Concentration-effect relationship of responses to simultaneous application of 10 nM isoproterenol (opened symbols) or vehicle (filled symbols) and increasing concentrations of A61603 ( $\blacksquare$ ,  $\square$ ) or NE ( $\bullet$ ,  $\circ$ ). Normalized fluorescence changes were recorded versus time. Dose-response data show peak fluorescence values over baseline. Plots represent one of four independent experiments, data points reflect the average values of duplicate samples.

**Panels E-H:** Kinetics of  $\text{Ca}^{2+}$  mobilization observed in HEK-293/EBNA cells transduced with control (**E**), wild-type  $\alpha_{1A}$ -AR (**F**), Ins\_ $\alpha_{1A}$ -AR (**G**) or Sub\_ $\alpha_{1A}$ -AR (**H**) baculoviruses exposed to 100 nM A61603 (blue) or 1  $\mu\text{M}$  NE (red), in the presence (dashed line) or absence (solid line) of 10 nM isoproterenol. The black solid line depicts the response to stimulation with 10 nM isoproterenol alone. Arrows indicate the time of agonist addition. Plots represent one of four independent experiments, data points reflect the average values of duplicate samples.

**Figure 6.** Potentiation of  $\text{Ca}^{2+}$  mobilization by 50  $\mu\text{M}$  forskolin or 50  $\mu\text{M}$  NECA in HEK-293/EBNA cells. Cells were transduced with control (**A, B**), wild-type  $\alpha_{1A}$ -AR (**C, D**), or Sub\_ $\alpha_{1A}$ -AR (**E, F**) baculoviral stocks. They were then stimulated with increasing concentrations of A61603 in the presence of vehicle (black squares), 50  $\mu\text{M}$  forskolin (green triangles) or 50  $\mu\text{M}$  NECA (red circles) (**Panels B, D&F**). Open symbols: effect of forskolin or NECA in absence of A61603. **Panels A, C & E:** Kinetic traces of calcium mobilization in response to forskolin (green) or NECA (red), in the presence (solid line) or absence (dashed line) of 100 nM A61603. The black solid line depicts response to stimulation by 100 nM A61603 alone and the grey solid line in Panel E corresponds to  $\text{Ca}^{2+}$  mobilization in response to

MOL #50765

stimulation with a combination of 100 nM A61603 and 10 nM Isoproterenol in Sub- $\alpha_{1A}$ -AR transduced cells. The agonist was added at the 10-second time point, as indicated by the arrows.

**Figure 7.** Effect of IP<sub>3</sub>R and CRAC inhibitors on Ca<sup>2+</sup> mobilization in response to A61603, in the presence or absence of 10 nM isoproterenol.

HEK-293/EBNA cells transduced with a wild-type  $\alpha_{1A}$ -AR baculoviral stock were pre-treated for 30 min with vehicle (black traces), or a combination of 5  $\mu$ M xestospongine C and 10  $\mu$ M 2-APB (red and blue traces). Cells were then stimulated with 100  $\mu$ M A61603 (blue and black traces) or 1 mM NE (red traces), in the presence (broken line) or absence (solid line) of 10 nM isoproterenol. Green traces represent control experiments employing untransduced cells pretreated with xestospongine C and 2-APB (light green, broken line: 100  $\mu$ M A61603 + 10 nM isoproterenol; dark green, solid line: 1 mM NE + 10 nM isoproterenol).

**Figure 8.** Deconvolution of the hypothetical kinetic components of the calcium signaling response initiated by  $\alpha_{1A}$ - and  $\beta_2$ -adrenoreceptors in HEK-293/EBNA cells.

**Panel A:**  $\alpha_{1A}$ -initiated Ca<sup>2+</sup> mobilization in response to activation of endoplasmic reticulum IP<sub>3</sub> receptors (maximum at 12 s after agonist addition). **B:**  $\alpha_{1A}$ -initiated, sustained Ca<sup>2+</sup> entry, likely due to the opening of store operated channels. **C:**  $\alpha_{1A}$ -initiated Ca<sup>2+</sup> mobilization in response to an unidentified signaling event (maximum signal at 23 s). **D:**  $\beta_2$ -AR initiated, cAMP-dependent Ca<sup>2+</sup>-mobilization, reaching a maximum at around 30 s. **Panels E & F** depict the interplay of the fast (red), intermediate (blue),  $\beta_2$ -AR initiated (green) and sustained (violet) components leading to the observed Ca<sup>2+</sup> transients in wild-type (**Panel E**) and Ins- $\alpha_{1A}$ -ARs (**Panel F**), upon co-stimulation with A61603 and isoproterenol. The black symbols (●) are actual traces observed

MOL #50765

with wild type (**Panel E**) or Ins\_ $\alpha_{1A}$ -ARs (**Panel F**) upon stimulation with A61603 plus isoproterenol. The arrows indicate the point of agonist addition.

MOL #50765

## TABLES

**Table 1.** Pharmacological parameters determined from IP accumulation and Ca<sup>2+</sup> mobilization assays performed with transiently transduced HEK-293-EBNA cells. Data were fitted to a sigmoidal dose-response equation using the GraphPad Prism software package to determine EC<sub>50</sub> and maximal response values.

	Agonist	EC <sub>50</sub> IP (μM)	EC <sub>50</sub> Ca <sup>2+</sup> (μM)	I.A. IP	I.A. Ca <sup>2+</sup>
Wild type α <sub>1A</sub> AR	NE	0.90 ± 0.20	0.070 ± 0.010	<sup>1</sup> 1.00	1.00
	A61603	0.040 ± 0.020	0.0027 ± 0.0006	1.07	0.86
Ins α <sub>1A</sub> AR	NE	4.0 ± 2.0	0.13 ± 0.05	1.00	1.00
	A61603	0.20 ± 0.10	0.0060 ± 0.0010	1.07	0.56
Sub α <sub>1A</sub> AR	NE	<sup>2</sup> BQL	BQL	BQL	BQL
	A61603	BQL	BQL	BQL	BQL
Untransduced	NE	BQL	0.50 ± 0.10	BQL	1.00
	A61603	BQL	BQL	BQL	BQL

<sup>1</sup>Intrinsic activity relative to NE

<sup>2</sup>BQL-Below quantifiable levels

MOL #50765

**Table 2.** Binding parameters.  $B_{\max}$  and  $K_d$  values determined from [ $^3\text{H}$ ]-Prazosin and [ $^{125}\text{I}$ ]-CYP saturation binding experiments performed with crude membranes derived from transiently transduced HEK-293-EBNA cells or stably transfected CHO- $\alpha_{1A}$  AR cells.  $K_i$  values were calculated from radioligand competition binding assays carried out with the same membranes. [ $^3\text{H}$ ]-Prazosin was used as a radioligand in competition assays with membranes derived from cells expressing  $\alpha_{1A}$  AR, while [ $^{125}\text{I}$ ]-CYP was used with membranes from parental and butyrate-treated HEK-293/EBNA cells.

Construct	$^3\text{H}$ -Prazosin		$^{125}\text{I}$ -CYP		NE $K_i$ ( $\mu\text{M}$ )	A61603 $K_i$ ( $\mu\text{M}$ )	Oxymet $K_i$ ( $\mu\text{M}$ )
	$K_d$ (nM)	$B_{\max}$ (fmol/mg)	$K_d$ (pM)	$B_{\max}$ (fmol/mg)			
HEK-293/EBNA	<sup>b</sup> NB	NB	46	11	<sup>a</sup> 34	<sup>a</sup> 729	<sup>a</sup> 185
HEK-293/EBNA NaBu-treated	NB	NB	65	274	<sup>a</sup> 24	<sup>a</sup> 1,161	<sup>a</sup> 265
HEK-293/EBNA $\alpha_{1A}$ AR	0.6	410±90	<sup>c</sup> ND	ND	3.1±1.0	0.13±0.02	0.031±0.009
HEK-293/EBNA Ins- $\alpha_{1A}$ AR	0.5	450±30	ND	ND	3.5±1.5	0.10±0.03	0.021±0.004
HEK-293/EBNA Sub- $\alpha_{1A}$ AR	0.6	650±90	ND	ND	7.7±2.4	0.17±0.07	0.032±0.013
CHO- $\alpha_{1A}$ AR	0.9	1070±50	ND	ND	1.5±0.4	0.05±0.01	0.013±0.03

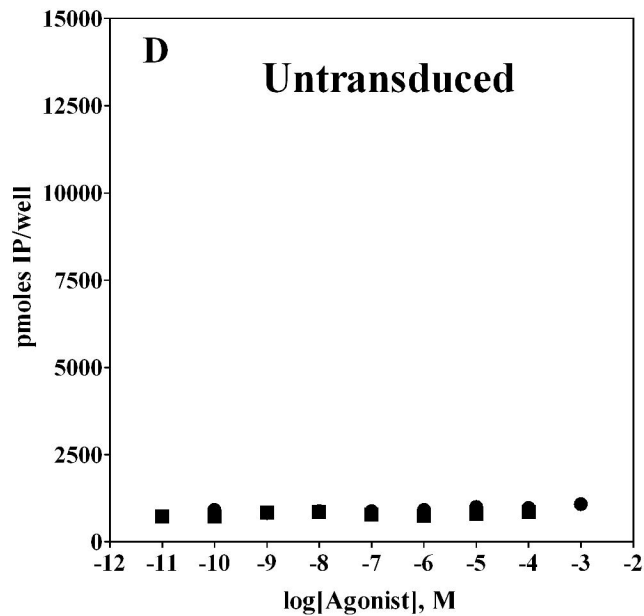
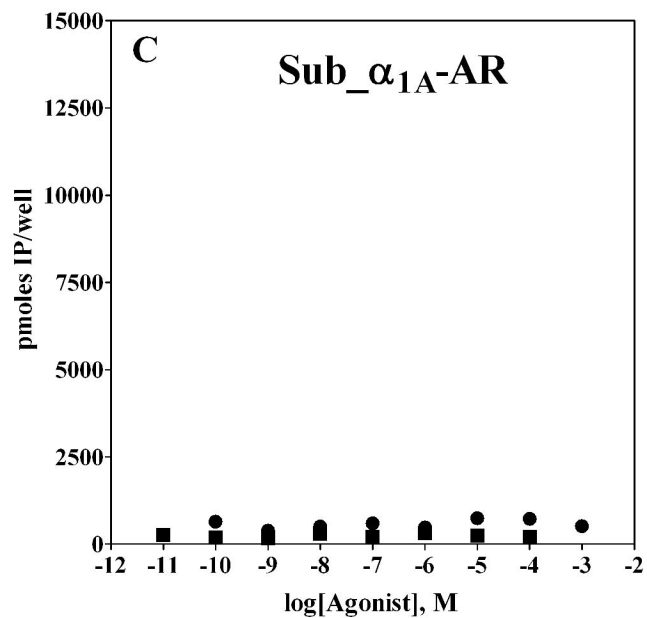
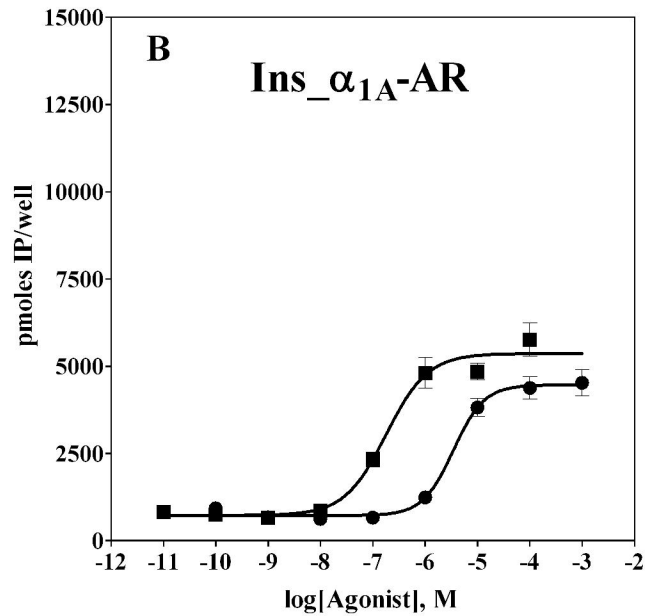
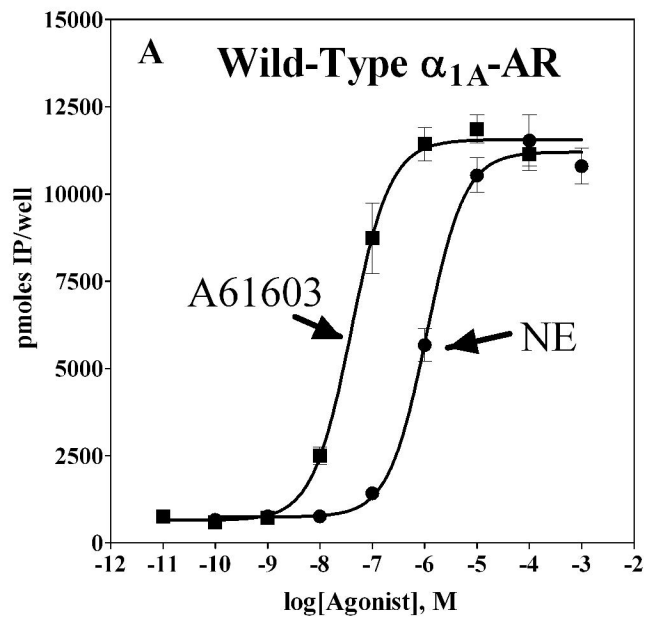
<sup>a</sup> [ $^{125}\text{I}$ ]-CYP used as a radioligand

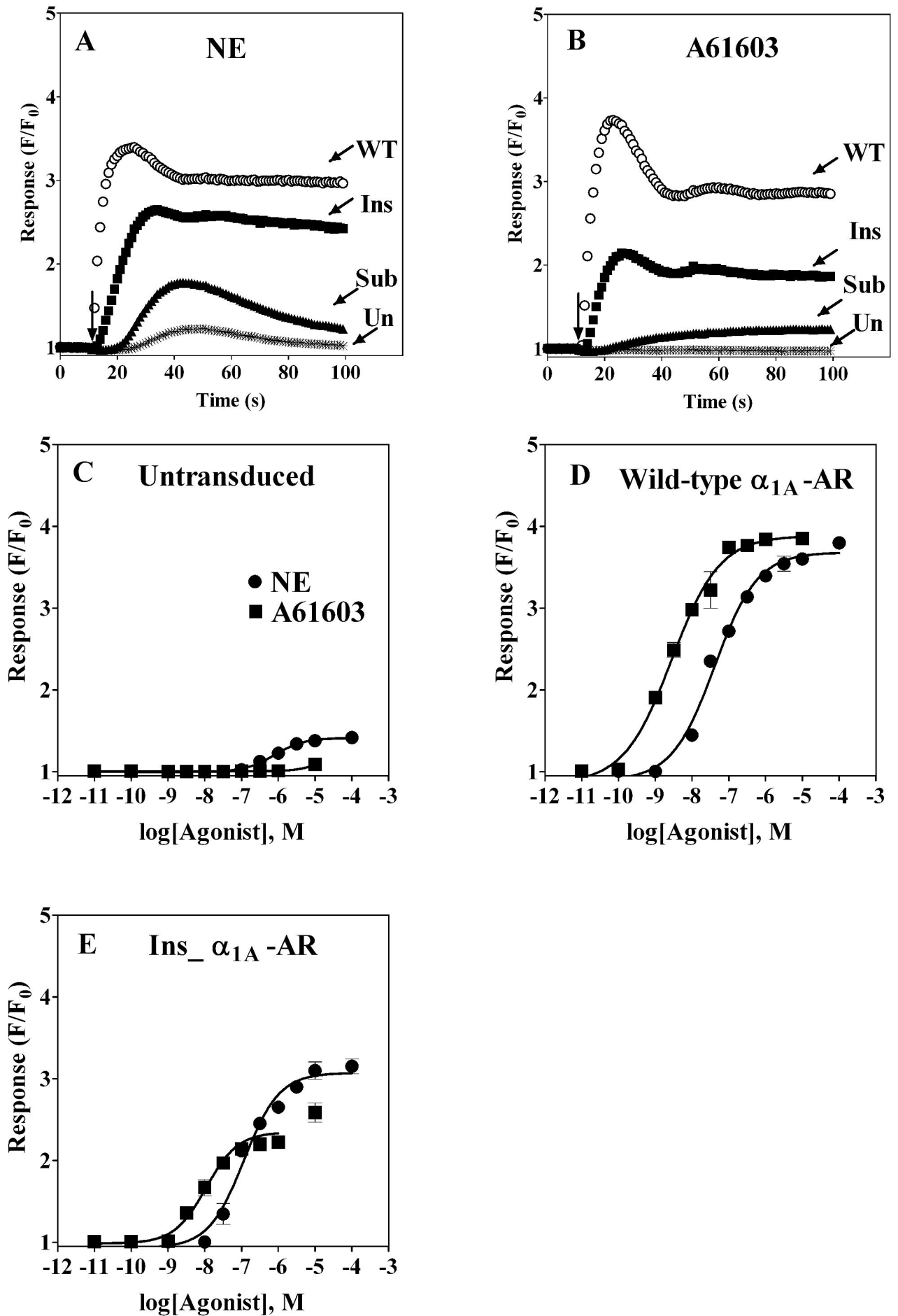
<sup>b</sup>NB-no detectable binding

<sup>c</sup>ND-not determined



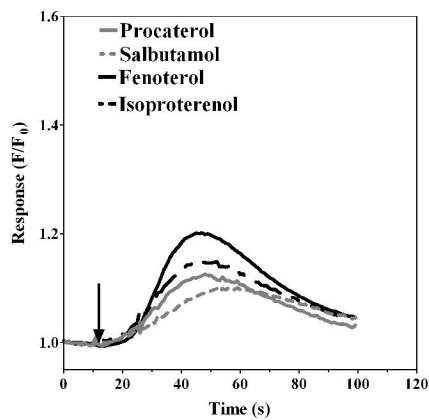
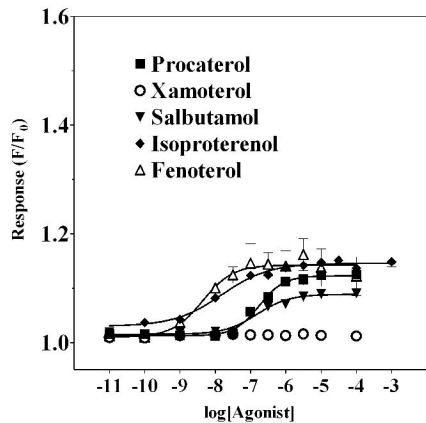
**FIGURE 1**



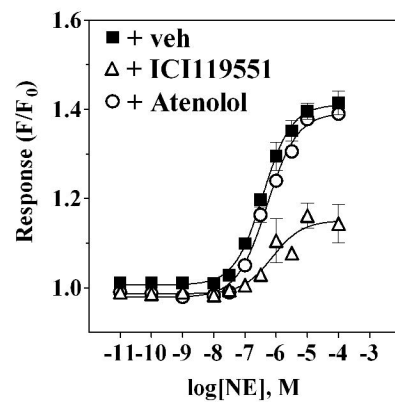
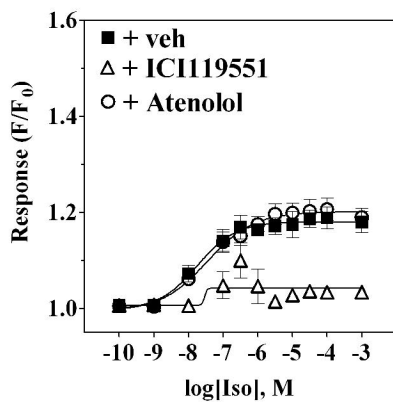
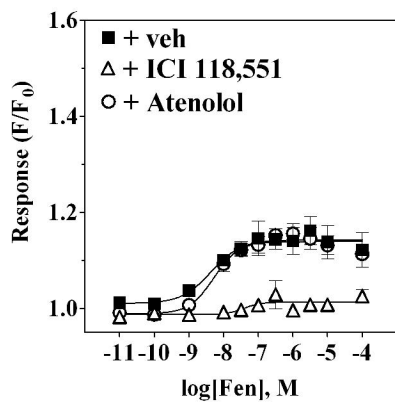
**FIGURE 2**

# FIGURE 3

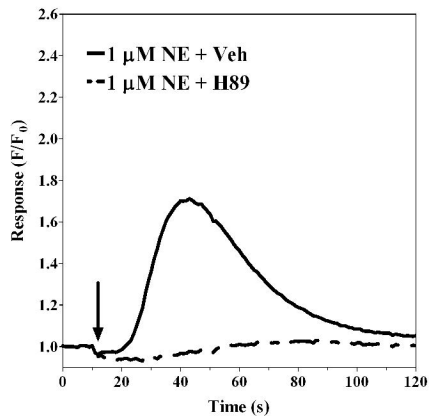
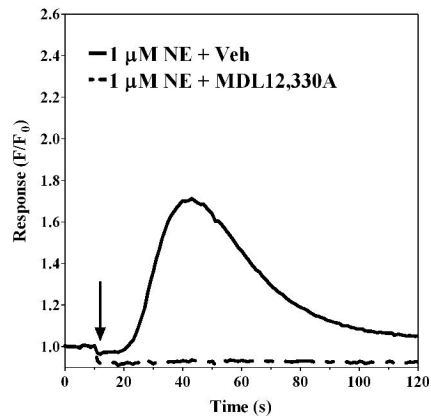
## A



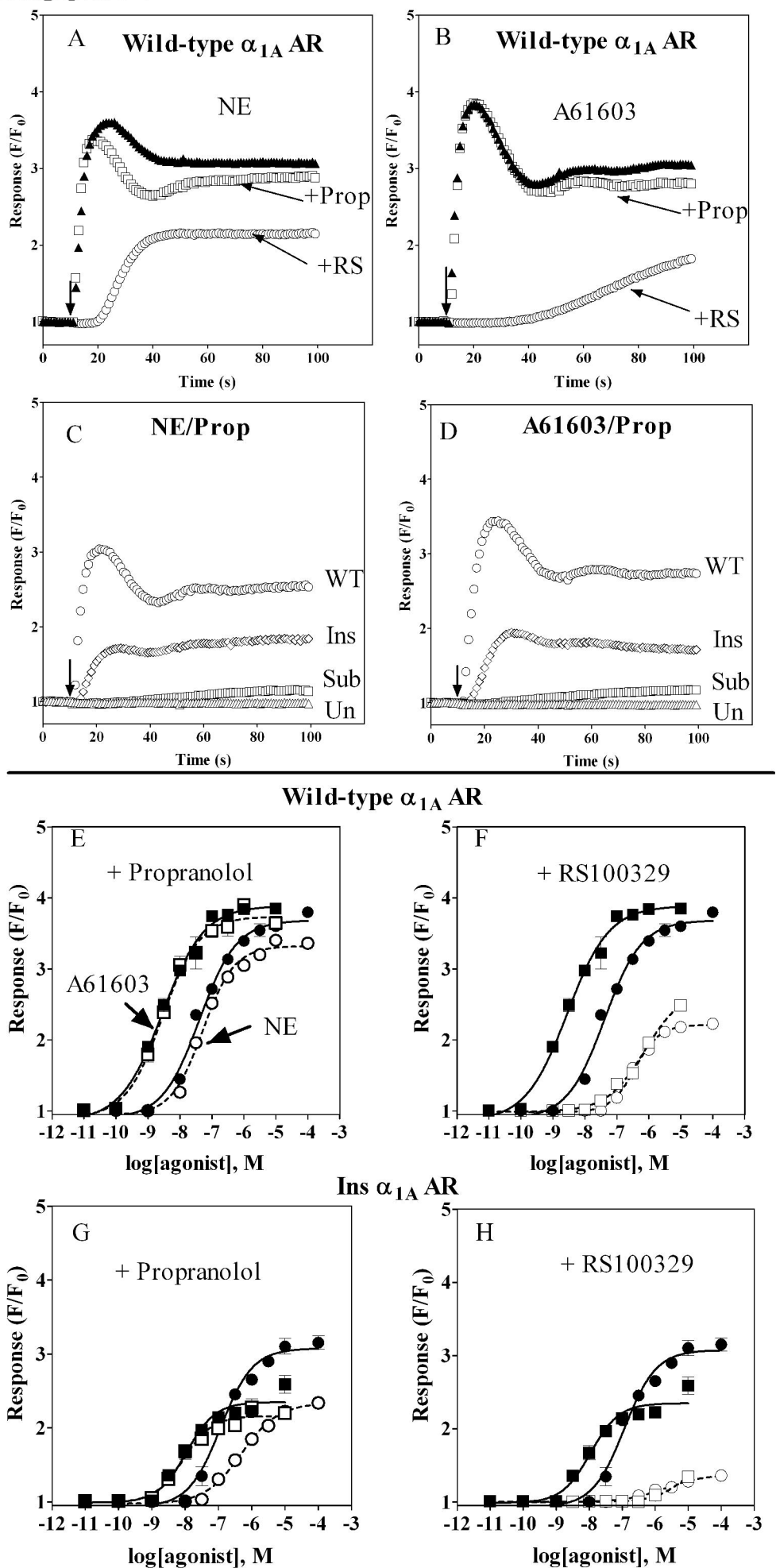
## B

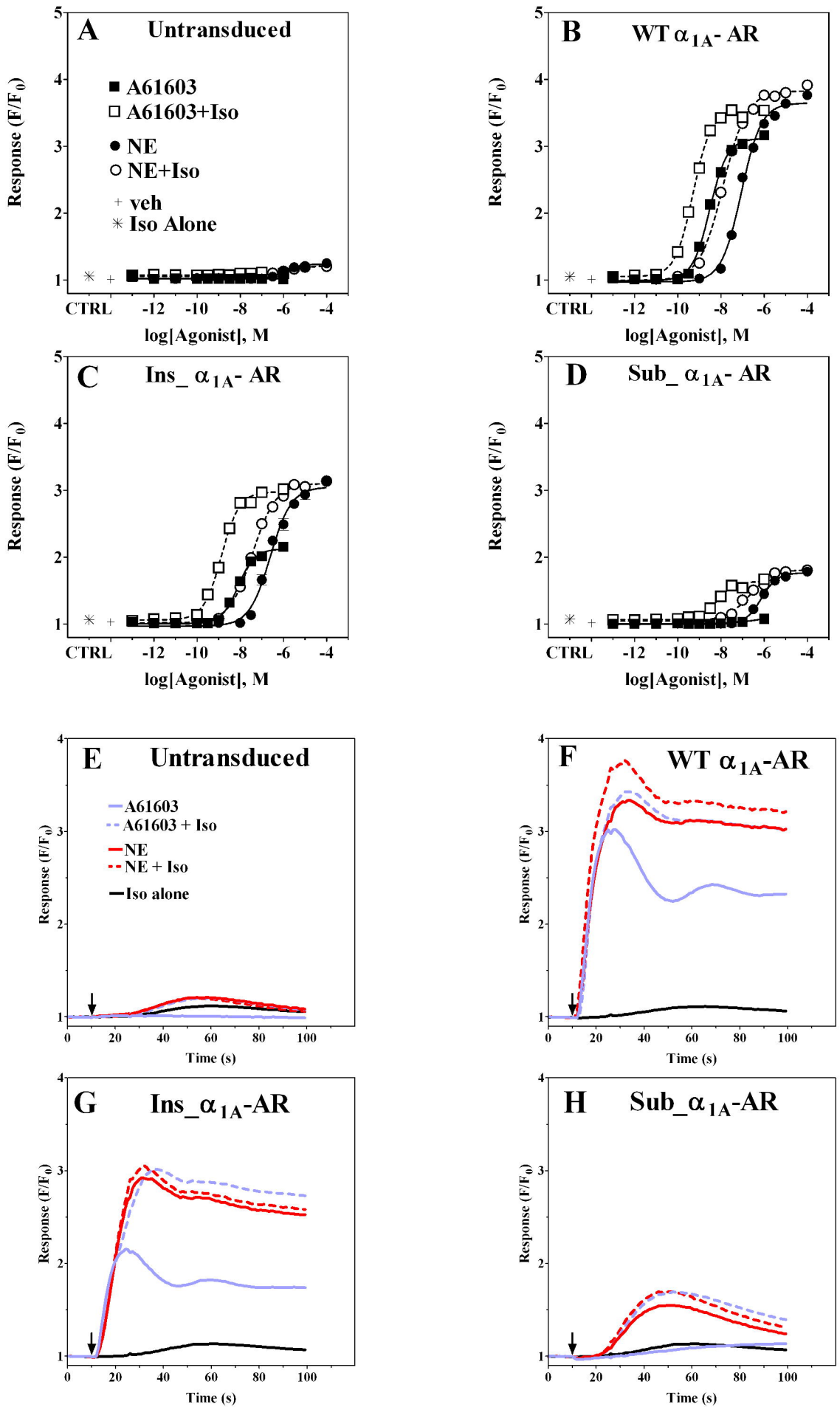


## C



# FIGURE 4



**FIGURE 5**

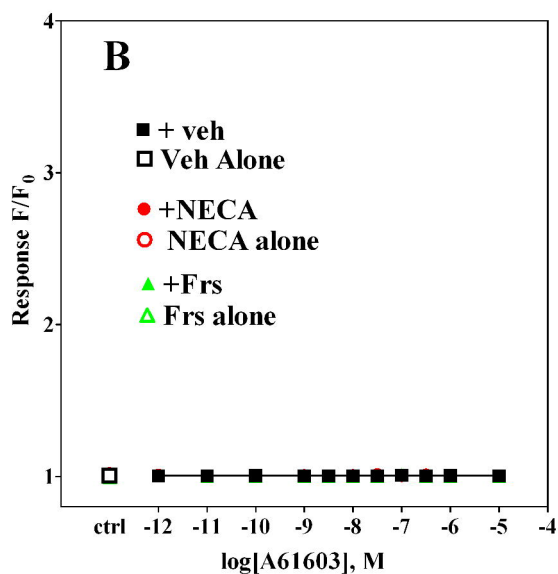
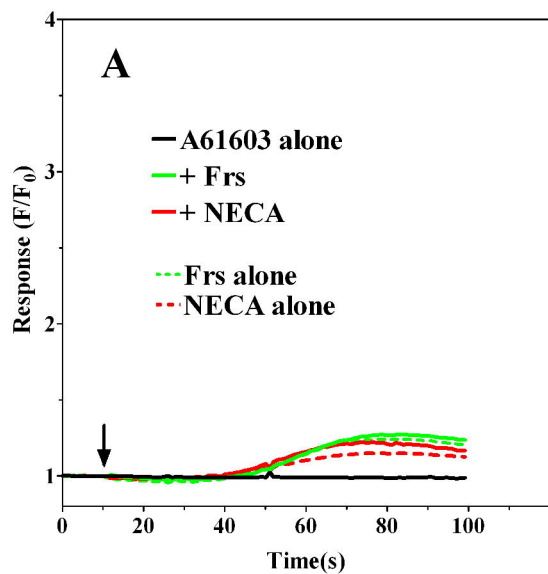
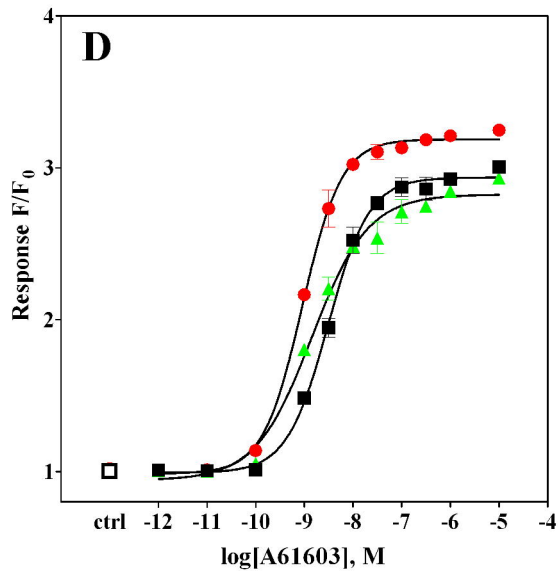
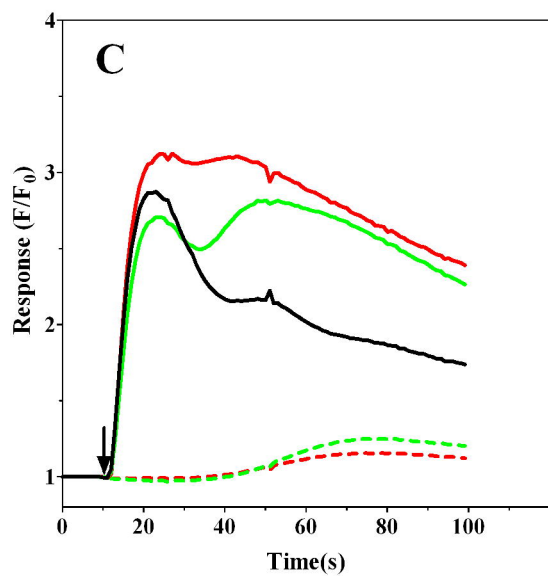
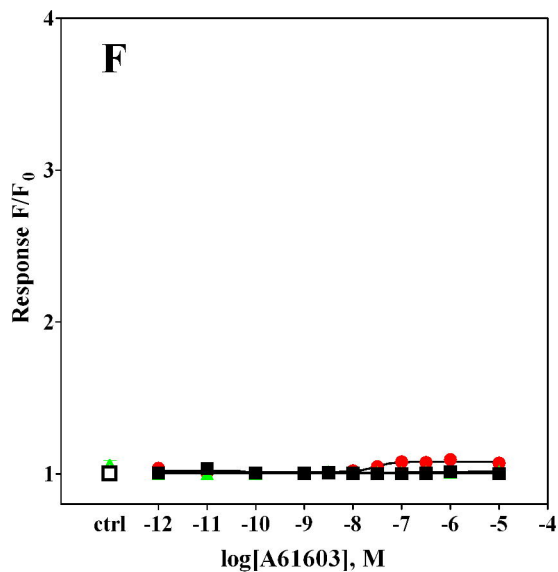
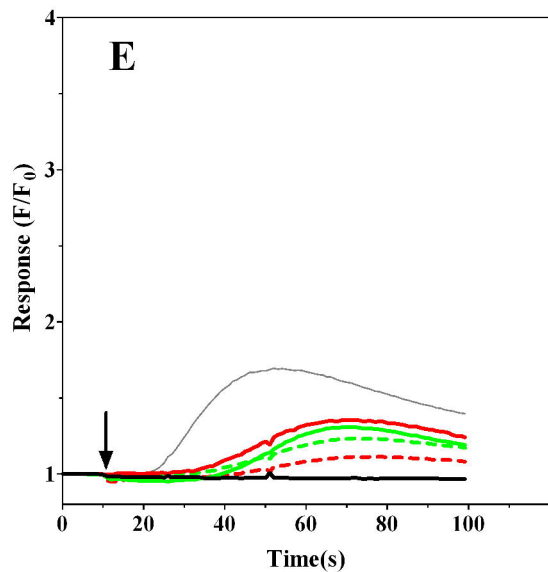
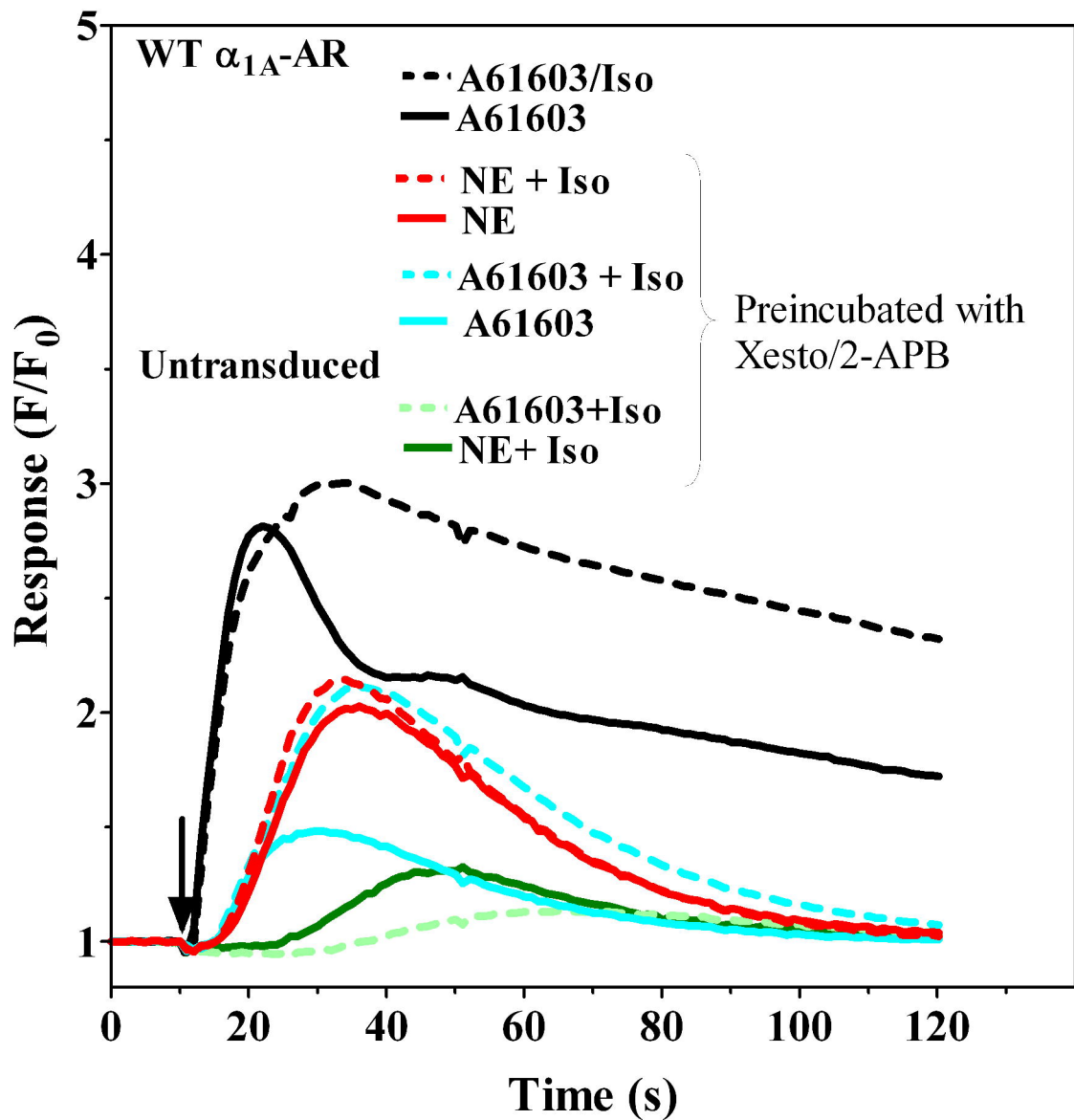
**FIGURE 6****Untransduced****wild-type  $\alpha_{1A}$ -AR****Sub\_ $\alpha_{1A}$ -AR**

FIGURE 7



# FIGURE 8

